both compounds was to focus on the relevancy of the number and quality of hemopoietic stem/progenitor cells and their significance in stem/progenitor cell kinetics in relation to leukemogenicity. Because an increase in radiation dose exponentially decreases the number of hemopoietic progenitor cells (Fig. 1A, line "a"), exposure to an ionizing radiation of >5 Gy will not yield a high frequency of leukemias, but will induce a significant decrease in the incidence of leukemias, possibly because of the decrease in the number of hemopoietic progenitor cells (although it remains unclear whether stem/progenitor cells are leukemic target cells). The minimum number of potentially mutated stem/progenitor cells for the development of one case of leukemia decreases with increase in radiation dose (Fig. 1A, line "b"). Thus, the integral of the shaded area shown in Figure 1 between those two functions may correlate to the risk of radiation-induced leukemias, although the scale of the ordinate for the stem/progenitor cell survival curve described here may be arbitrary. Namely, the shaded shared area between the area beneath the stem/progenitor cell survival curve and the upper area of the lower curve, i.e., the minimum number of mutated stem/progenitor cells for the development of one case of leukemia as a function of radiation dose, may be the risk factor for radiation-induced leukemogenesis. Furthermore, when one incorporates corresponding data from p53-knockout mice (Fig. 1B) and other data from genetically modified animals, any modifications of shared areas suggest a decrease and/or an increase in risk of the incidence of experimental leukemogenesis. Such statistical relevance between the number of hemopoietic stem/progenitor cells and the induction of experimental leukemias can be applied also to the study of the incidence of benzene-induced leukemias. In the case of benzene-induced leukemias, the relevance of stem cell kinetics to the incidence of experimental leukemias is a function of changes in hemopoietic progenitor cells. In this article, such relevancies between the number and quality of stem/progenitor cells and the incidence of leukemias after radiation and/or benzene exposure with respect to biological modification after caloric restriction and/or modification of the state of oxidative stress are introduced after a brief description of the characteristics of hemopoietic progenitor cell function.

Materials and methods

Mice

C3H/He and C57BL/6 strain, male and female, with or without genetic modification for p53 deficiency [4] or thioredoxin overexpression [5] were used in the hemopoietic stem/progenitor cell research, radiation- or benzene-induced leukemogenesis followed by histopathological examination. Experimental animal protocols used were reviewed by the externally established peer-review panel, and maintained in the board-approved laboratory animal facility of the National Institute of Health Sciences of Japan.

Radiation and bone marrow transplantation

For a lethal dose of radiation (9.45 Gy) for bone marrow transplantation and a graded increased dose up to 5.0 Gy of x-ray irradiation for induction of hematopoietic malignancies, mice were subjected to a 200-kV/20 A pulse through a therapeutic x-ray irradiator (Shimadzu, Tokyo) with 1.0-mm aluminum and 0.6-mm copper filters, at a dose rate of 0.614 Gy/minute and a 56-cm focus surface distance. Whole-body irradiation (8.5 Gy) by gamma-ray

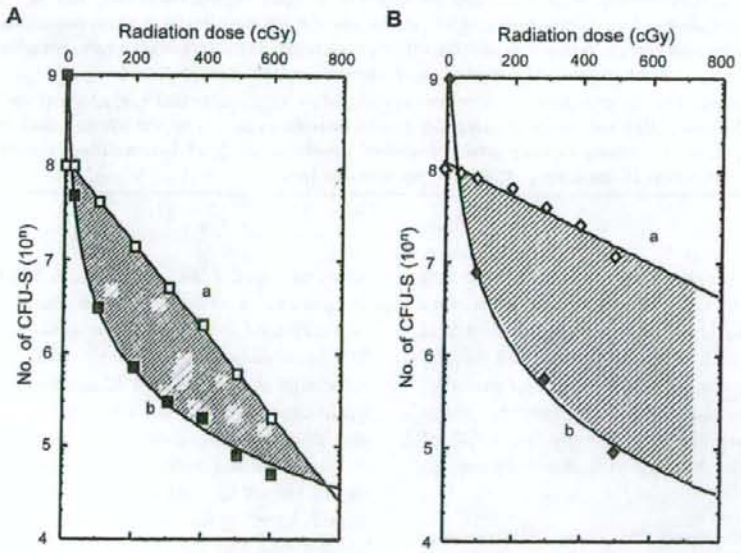

Figure 1. Possible risk of radiation-induced leukemia in wild-type mice (**A**) and p53-homozygous knockout mice (**B**). (**a**) Survival of stem cells after irradiation. (**b**) Minimum number of stem cells for development of a case of leukemia.

^{137}Cs, at a dose rate of 0.101 Gy/minute, Gammacell 40 Exactor; IDS Nordion, Ottawa, Canada) with a 0.5-mm aluminum-copper lter was also given in the assay of colony-forming unit in spleen.

enzene and benzene exposure

enzene (CAS no. 71-43-2, MW 78.11) was purchased from /ako Fine Chemical Company (Osaka, Japan). Mice were ran-omly assigned to groups and individually housed. They were xposed to benzene in 1.3 m^3 inhalation chambers as described reviously [6,7]. The benzene-exposed mice were exposed to 00 ppm of benzene 6 hours per day, 5 days per week for 2 weeks r short-term examination, and 26 weeks for leukemogenicity ioassay. The mice were supplied water ad libitum, but food pel-ts were withdrawn during the exposure.

'aloric restriction

or caloric restriction studies, a 77 kcal/week was maintained. iroups subjected to different caloric restriction timings were com-ared with groups not subjected to caloric restriction during life-me for incidences of neoplasms followed by histopathological xamination [8,9].

ssays for CFU-S and CFU-GM

or assay of hematopoietic colonization, colony-forming unit in pleen (CFU-S) [10] and colony-forming unit granulocyte macro-hages (CFU-GM) [7,11] were evaluated. For CFU-GM assay, semisolid methylcellulose culture, supplemented with 10 ng/ iL murine granulocyte macrophage colony-stimulating factor R&D Systems, Inc., Minneapolis, MN, USA) was conducted.

UUV method

lematopoietic progenitor cell-specific kinetic studies were evalu-ted by continuous labeling of bromodeoxyuridine for cycling ells, followed by UV exposure and hemopoietic colonization BUUV method, details in [11,12]).

'ompertzean expression

xperimental survival curves were applied to Gompertz's law of iortality to examine lifespans and mortality rates in mice with nizing radiation- and benzene-induced leukemias. (Detailed pro-edure of mathematical analysis by Gompertz-Makeham law of iortality is found in ref. [1].).

tesults and discussion

lemopoietic stem/progenitor cells
s a target of experimental leukemogenesis

iecause the major histopathological type of radiation-nduced leukemia in p53-deficient mice was stem cell leu-emia with trace evidence of myeloid differentiation, the ossible target cells in leukemogenesis were supposed to e hemopoietic stem/progenitor cells [13]. Interestingly, 53-heterozygous deficiency also produced stem cell leuke-ia with loss of heterozygousity after graded increased oses of radiation exposure (unpublished observation). herefore, to understand the mechanism underlying leuke-iogenesis induced by radiation and/or benzene exposure, urrent series of evidence regarding stem/progenitor cell characteristics are particularly important. Furthermore, in addition to the generation-age structure of hierarchic stem/progenitor cells, current knowledge on genes regulating kinetics in stem/progenitor cells (i.e., genes maintaining the long-term repopulating cells), genes in splenic colony-forming units, and genes in in vitro colony-forming units, is found to be particularly important for understanding development of leukemias. Because of the possible participation of negative regulators of stem/progenitor cell differentiation and self-renewal, such as *Notch* [14], *Wnt* [15], and *Sonic hedgehog* [16] signals, and *Bmi-1* [17] expression, a dormant fraction, about 80% in the hemopoietic stem/progenitor cell compartment, which does not incorporate bromodeoxyuridine (BrdUrd), is continuously maintained for lifetime after the development of this dormant fraction during the neonatal stage. The cycling fraction, on the other hand, incorporates BrdUrd continuously and about 20% of the total progenitor cell compartment is maintained throughout the lifespan. Furthermore, the doubling time of each progenitor cell compartment in the stem/progenitor hierarchy is facilitated in the order from immature progenitor cells with faster generation time to mature progenitor cells with slower generation time (data not shown). The size of dormant fractions slightly decreases with the age structure of progenitor cells. We previously observed that hemopoietic progenitor cells also maintain their immaturity with transforming growth factor-β (TGF-β) [18], as well as gap junctional intercellular communication, specifically with connexin-32, which was supposed to maintain the size of the immature stem/progenitor cell compartment, steady-state growth, regenerating potential after experimental chemical abrasion, and possibly function as a tumor suppressor for leukemogenesis.

Novel tool to evaluate
hemopoietic progenitor-specific cell kinetics
(BUUV method[1]) as a key parameter for leukemogenesis

The concept of a stem/progenitor cell pool and the daily outflow (i.e., production) of committed cells to erythropoietic, granulopoietic, and megakaryocytic lineages were also intensively studied by Cronkite and his associates from the 1960s to the 1970s. They determined the number of stem/progenitor cells undergoing DNA synthesis using tritiated thymidine (^{3}H-TdR) with a low specific radioactivity as well as the incorporation of ^{3}H-TdR with a cytocidal dose of high-specific activity for evaluating the cycling fraction [19]. In the early 1980s, Cronkite applied his knowledge on steady-state hematopoiesis to toxicological studies, not only to the radiation-induced, but also benzene-induced, hemopoietic toxicities and their consequence, namely,

[1]Continuous infusion of bromodeoxyuridine by osmotic minipump to label cycling cells in general is carried out, followed by UV exposure to kill labeled cells, and then allowing surviving stem cells to form hemopoietic colonies.

leukemogenesis [20]. Cell kinetic studies using ^{3}H-TdR with low- and high-specific activities provided a new paradigm of benzene- and other chemical-related hematotoxicities.

There are two technical limitations of the experimental and hematological use of ^{3}H-TdR. First, ^{3}H-TdR with a low-specific activity enables labeling of cycling cells, but not killing them, second, ^{3}H-TdR with a high-specific activity, enables the labeling and killing of cycling cells, but not the studying of long-term cell kinetics. The BUUV method established by Hirabayashi and coworkers [11,12] entails the purging of cells labeled by BrdUrd using UV-A light for evaluating the kinetics of hemopoietic progenitor cells, followed by colonization and other hematological evaluations (Fig. 2). The method enables long-term labeling of cycling cells for up to nearly a lifetime and the assay of the size of the cytocide fraction at anytime by exposure to UV-A light followed by relevant colonization assay methods and/or cell sorting. Although many similar methods were reported previously, none of them are appropriate for hemopoietic stem cell research. The reasons are as follows: In previous methods, UV-B and UV-C lights were used, not UV-A light, which resulted in serious errors. In the case of Pietrzyk et al. [21], they used highly toxic UV-C light, which that made progenitor cells mortal regardless of the labeling, and thus, made a real dormant fraction missing. In the case of Hagan and colleagues [22,23], they used UV-B light, and found plateau phases of a surviving colony fraction with increasing dose of UV-B fluence (J/m^2) after increasing the period of BrdUrd infusion. The fraction containing cycling one measured on the basis of colony formation still exponentially increases >90%. Use of UV-A and incorporation of BrdUrd in drinking water for long-term administration collaboratively provided a revolutionary paradigm for increasing the knowledge of kinetics in the hemopoietic stem/progenitor cell compartment.

A new discovery is the existence of a long-term and stable, dormant fraction. This is similar to crypt stem cells at the bottom of intestinal villi, described by Potten et al. [24], but never clearly observed in the hemopoietic system. The dormant fraction develops presumably after the early developmental stage of the neonatal period, which forms an orderly generation-age structure from a primitive CFU-S-13, mature CFU-S-9, and to an in vitro CFU-GM (21.7% ± 4.7%, 33.4% ± 3.3%, and 35.0% ± 3.7%, respectively [11]). Second, by BUUV assay, some disadvantages of in vitro labeling with ^{3}H-TdR and also with BrdUrd were consequently discovered; e.g., in vitro labeling artificially results in a marked overestimation of the percentage of the labeled fraction from 9.9% ± 4.8% to 37.4% ± 4.5%. The cycling fraction of CFU-GM is often labeled and assayed in vitro. The in vivo labeling assay value is

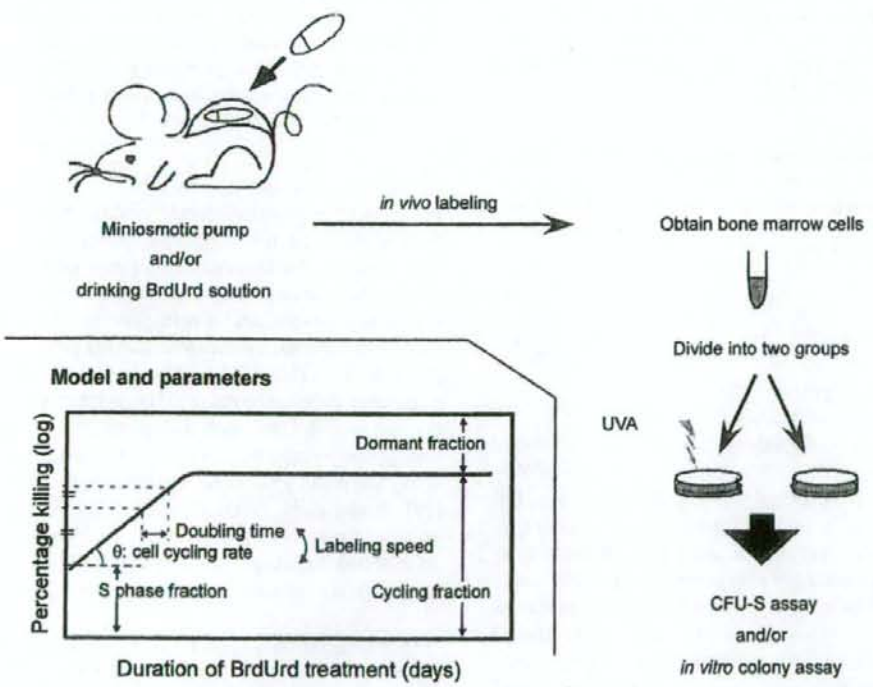

Figure 2. Bromodeoxyuridine UV method as a tool for evaluating size and other parameters of cycling stem cell fraction in vivo [12].

nly slightly higher than the actual CFU-S cycling fraction hen assayed by in vivo labeling, regardless of the labeling nethod; that is, intravenous injection or via drinking water 9.9% ± 4.8% vs 6.8% ± 4.8%; CFU-GM vs CFU-S-9, re-pectively). Many previous studies showed that CFU-GM nd other in vitro colonies labeled with ^{3}H-TdR cytocide vere nearly 60% in cycling, which was used as an indicator f the maturity of progenitor cells in vitro in terms of gen-ration age, but are now considered artifacts.

The doubling time and the generation time of each pro-enitor cell compartment are also dependent on the age-tructure, and the doubling times are from 35.2 hours in FU-S-13, 48.5 hours in CFU-S-9 to 56.0 hours in CFU-M, respectively [11]. For example, in the cases of caloric striction and 3′-azido-3′-deoxythymidine treatment, both arkedly decreased the cycling fraction of the hemopoietic em/progenitor cell compartment [8,9,25].

adiation-induced leukemogenesis
nd its prevention by caloric restriction

s shown in Figure 1A, the incidence of radiation-induced ukemias depends on two functions: one is stem/progenitor ell survival with graded increases in radiation dose and the ther is the minimum number of potentially mutated stem/ rogenitor cells for the development of one case of leuke-ia vs graded increases in doses of radiation. Because e integral of the shaded channel area in Figure 1 de-eases with the increase in radiation doses and the channel closed at 6 to 7 Gy, radiation-induced leukemias are not pposed to develop at more than 6 to 7 Gy in the murine stem. In the case of p53-deficient mice, however, despite diation-induced damage, the survival of hemopoietic pro-nitor cells with the increase in radiation dose shows much shallower survival curve (Fig. 1B, line "a"), owing their escape from p53-dependent apoptosis; these cells ay retain unrepairable DNA damage (data not shown; 3,26]). This modification of the survival curve of hemo-ietic stem/progenitor cells deficient in p53 further in-eases the incidence of radiation-induced leukemias, and e incidence of leukemias following 5-Gy exposure keeps creasing up to 100% (unpublished data).

Next, we modified radiation-induced leukemogenesis by loric restriction, because caloric restriction is the only nu-tional factor that extends lifespan of experimental ani-als [27], and is supposed to attenuate radiation-induced ukemias [9]. The C3H/He mouse strain shows a high cidence of myeloid leukemias, with a low spontaneous cidence (of myeloid leukemia). Nonirradiated mice owed a 1% incidence of spontaneous myeloid leukemias th a median lifetime of 839 days. The incidence of mye-d leukemias increased up to 22.2% with a decrease in dian lifetime to 697 days after the 3-Gy whole-body ay irradiation of mice. Various methods of caloric re-iction induced a prominent decrease in the incidence of eloid leukemias at 3 Gy; i.e., 9.5% in the group with caloric restriction for the rest of their lifetime immediately after the irradiation; 8.0% in the group with caloric restriction throughout their lifetime. No leukemia developed in groups not exposed to radiation (data not shown; [9]).

Along with the decrease in the incidence of myeloid leukemia in the group with caloric restriction, interestingly, the percentages of tumor-free mice consequently increased from 7.4% to 17.5% and 20.0%, in the group with caloric restriction for the rest of their lifetime after 3-Gy irradiation and in the group with caloric restriction throughout their lifetime, respectively. Nonirradiated group with caloric restriction also showed a statistically significant increase 10.1% to 46.4% in the percentage of tumor-free mice as compared with groups without caloric restriction.

Because caloric restriction decreased the number of hemopoietic stem/progenitor cells and the cycling fraction of hemopoietic progenitor cells, as evaluated by the BUUV method in these series of experiments, we conclude that caloric restriction decreases the incidence of radiation-induced leukemias via two mechanisms. First, the suppression of direct genotoxic leukemogenesis during the initiation stage, i.e., caloric restriction started before irradiation and continued until irradiation. Second, the suppression of indirect epigenetic leukemogenesis during the promotor stage, i.e., restriction started after irradiation and continued for lifetime. In these studies of caloric restriction, particular attention was focused on the number and cell cycle of hemopoietic stem/progenitor cells regardless of other suppressive factors that may also contribute to general oncogenesis, such as oncogene expression, DNA methylation, free radical formation, apoptosis induction and immunity activation, among others.

Benzene-induced hemopoietic
toxicities and induction of leukemias,
and their attenuation by thioredoxin overexpression

Cronkite was the first scientist who clearly recognized the relevance of the number and position of hemopoietic stem/progenitor cells in their kinetics with respect to the development of leukemias [28]. Consequently, his benzene exposure protocol successfully induced the first experimental benzene-induced leukemias; namely, the induction of a modest decrease in the number of hemopoietic progenitor cells that does not lead to extinction of such cells [2], which was after the first report of leukemogenicity induced in humans nearly 80 years ago [29]. He was interested in, and focused on, peculiar oscillatory changes in the numbers of bone marrow cells and hemopoietic progenitor cells, although laborious ^{3}H-TdR labeling for the complicated cell-cycle perturbation induced by benzene exposure could not help his group clarify the mechanism underlying cell-cycle oscillation. As reported by our group previously in *Experimental Hematology* [7], benzene exposure was found to be not only in mature blood cells, but also in hemopoietic stem/progenitor cells, a strong cell-cycle suppressor, due to clastogenic

damages suggested by an upregulation of topoisomerase III in the bone marrow [30]; however, cessation of benzene exposure during weekends induced rapid recovery of the cycling of the hemopoietic stem/progenitor cell fraction, which induced the repeated counter-oscillatory changes during the exposure period and resulted in a high frequency of epigenetic induction of hemopoietic malignancies (Fig. 3). Benzene and its major metabolites are negative in Ames-revertant mutagenesis assay, and induce a lesser amount of DNA adducts, which cannot explain in detail the mechanism underlying leukemogenicity. Benzene-induced cell-cycle perturbation observed in the present study may collaboratively cause clastogenic chromosomal damage induced by benzene mono-oxide and oxidative stress [30,31].

Conclusion from the base of bioinformatics: Experimental leukemogenesis and its attenuation with respect to related changes in Gompertzean survival curve

In the theoretical model of the mortality rate of human beings, studied by Gompertz [1] more than 180 years ago, he found that death rate during a unit time interval increases exponentially with lifetime. The Gompertzean expression can be applied to major mammalian species (Fig. 4A) [32]. The implication of Gompertzean linearity in experimental groups and changes in the slope linearity are considered to be based on an observation that lifespan may involve a function based on the multiplication of various life-threatening factors. Namely, the linearity is based on a system in which each lifespan-linked disease is independent and links to other diseases multiply (Eq. 1).

$$N'(t) = -rN(t)\log(N(t)/K) \quad (1)$$

where $N(t)$ is number of individuals at time t, r is intrinsic growth rate, and K is number of individuals in equilibrium.

Furthermore, any continuous life-threatening factors except deaths from traffic accident, war, or epidemic infections, make Gompertzean linearity steeper (Fig. 4B: standard, "Std", to "Tox"). For example, in the case of mice exposed to graded increases in radiation dose, their lifespan shows continuously steeper curves from high-dose to zero-dose group, i.e., a steeper curve to a shallower

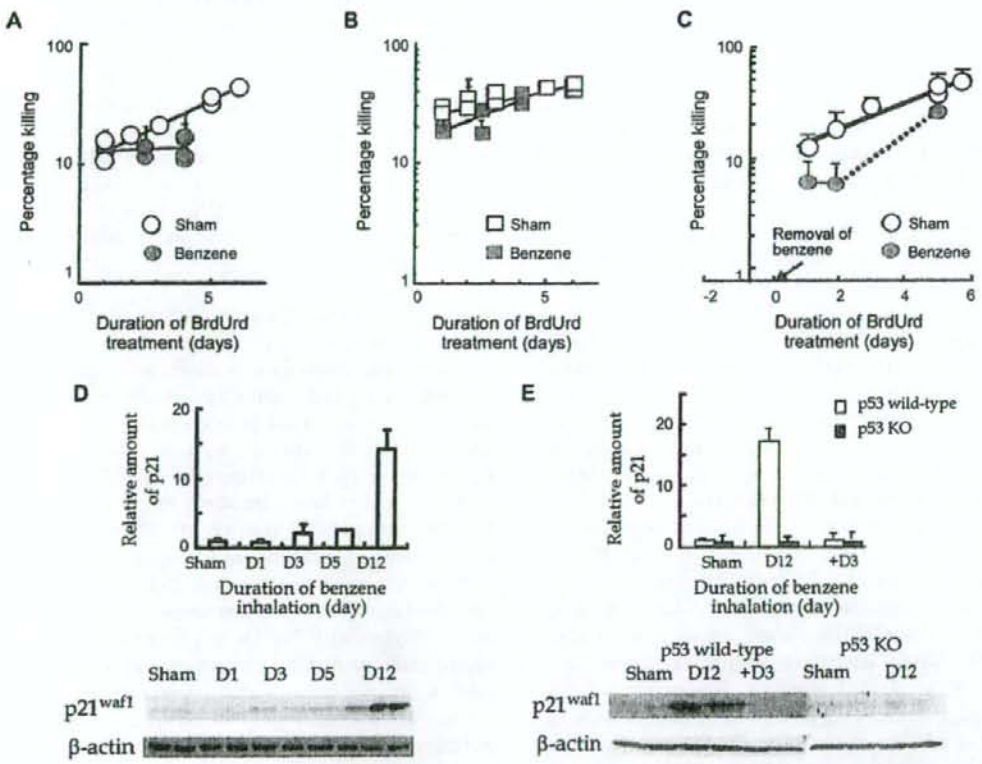

Figure 3. Benzene-induced cell-cycle arrest via p53-p21^{waf1} signal pathway [7]. (**A**) In wild-type mice, cell kinetics is stopping during the benzene inhalation (closed circles) vs sham control (open circles). (**B**) In p53-homozygous knockout mice, cell kinetics is maintained during benzene inhalation (closed squares) vs sham control (open squares). (**C**) After stopping benzene exposure, cell kinetics rapidly recovers in wild-type mice. (**D**) In wild-type mice, p21^{waf1} is upregulated during benzene inhalation. (**E**) In p53-homozygous knockout mice, p21^{waf1} is not changed during benzene inhalation. After stopping benzene inhalation, in wild-type mice, p21^{waf1} is downregulated immediately.

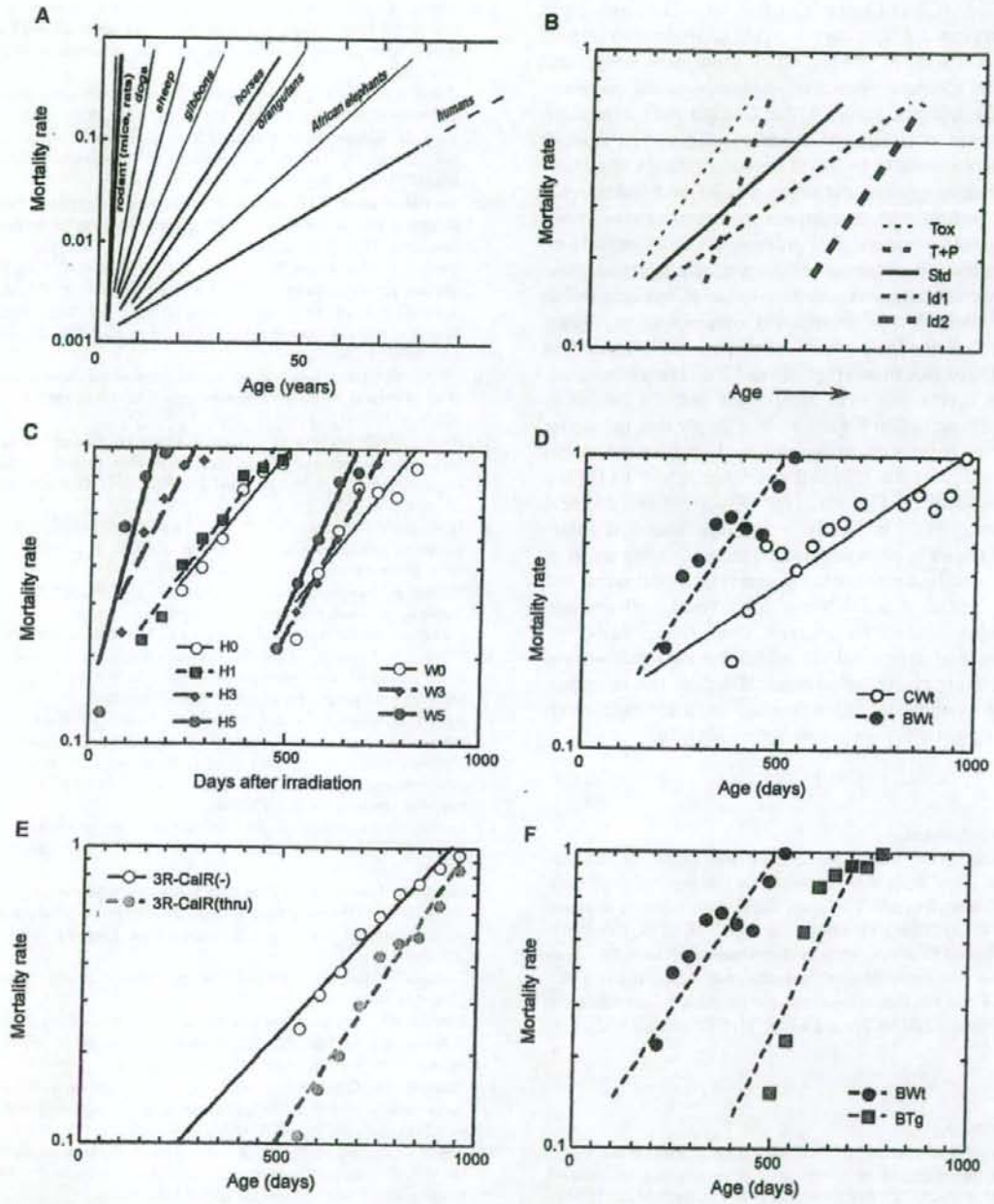

4. Gompertz's low of mortality was applied to examine lifespans and mortality rates in mice with ionizing radiation (IR)- and benzene-induced ıias. (**A**) Lifespan in the steady-state animals, based on the life expectancy. (**B**) Gompertz model for lifespan in toxic changes and its attenuations. toxic state; T+P = toxic state with prevention; Std = standard; Id = ideal state). (**C**,**E**) Radiation-induced shortening of lifespan. (**C**) H0 to H5 heterozygous knockout mice with 0 to 5 Gy whole-body irradiation; W0 to W5 = wild-type mice with 0 to 5 Gy whole-body irradiation and its y by caloric restriction. (**E**) 3R-CalR(−); 3-Gy irradiation without caloric restriction, 3R-CalR(thru); 3-Gy irradiation with caloric restriction). Av- aloric intake calculated was 77 kcal per week per mouse (i.e., 81.1% of the nonrestrict control). Detailed technical information for caloric restriction found elsewhere [9]. (**D**,**F**) Benzene-induced shortening of lifespan. (**D**) CWt = wild-type mice for sham control; BWt = wild-type mice with benzene re) and recovery by Trx overexpression. (**F**) BWt = wild-type mice with benzene exposure; BTg = thioredoxin overexpression mice with benzene re. Benzene was exposed at 300 ppm, 6 hours per day, 5 days a week, for 26 weeks. For Trx overexpression mice, detailed technical information can be lsewhere [5,31].

curve (Fig. 4C). In Figure 4C, H0 through H5 indicate p53 heterozygous-deficient mice exposed to graded increases in dose of radiation (0–5 Gy), which show more steeper and shortened lifespans. Similarly, benzene-induced leukemias make the lifespan curve in the Gompertzean expression also steeper with benzene exposure (Fig. 4D). Although these slopes seem to be based on the incidence of various types of tumorigenesis, the slopes may be modified by other chronic factors, such as nutrition related to cardio- and/or renal-vascular diseases. Two prevention studies provide interesting prevention curves in Gompertzean expression; one on caloric restriction in radiation-induced leukemogenesis [9] and the other on thioredoxin overexpression against benzene toxicity [31], which shows potentially equivalent antioxidative functions (Fig. 4E and F). Gompertzean expression curves for toxic compounds and for inhibitory compounds shown in Figure 4C to F imply that the slopes for Gompertzean expression may be based on the model shown in Figure 4B (Fig. 4E corresponds to "T+P (Tox & Prevention)" in Fig. 4B; Fig. 4F corresponds to ideal prevention, "Id 2" in Fig. 4B.). The significance of differences in slopes in Gompertzean expression among the non-treated animals, animals treated with toxic compounds, and animals treated with inhibitory compounds, and possible deterministic factors for genomic stabilization, cell-cycle regulators and active caloric metabolic enzymes, among others, are not clearly understood. However, this relevance would be an important factor for elucidating the mechanism underlying toxicities vs prevention of lifespan.

Acknowledgments

The authors would like to thank the collaborators for valuable assistance. This work was supported in part by the fund from Nuclear Research of MEXT, Japan, the Human Sciences of Japan (KH31034, KHC1204), Grants-in-Aid (Nos.13670236, 15510064, 16590329 and 18510066) for Scientific Research C from the Japan Society for the Promotion of Sciences, and Risk Analysis Research on Food and Pharmaceuticals for Health and Labor Science Research Grants (H15-Chemicals-002, H16-Chemicals-002).

References

1. Gompertz B. On the nature of the function expressive of the law of human mortality, and on a new mode of determining the value of life contingencies. Pholos Trans Royal Soc (Lond). 1825;115:513–585.
2. Cronkite EP, Inoue T, Carsten AL, Miller ME, Bullis JE, Drew RT. Effects of benzene inhalation on murine pluripotent stem cells. J Toxicol Environ Health. 1982;9:411–421.
3. Cronkite EP. Hemopoietic stem cells: an analytic review of hemopoiesis. Pathobiol Annu. 1975;5:35–69.
4. Tsukada T, Tomooka Y, Takai S, et al. Enhanced proliferative potential in culture of cells from p53-deficient mice. Oncogene. 1993;8:3313–3322.
5. Mitsui A, Hirakawa T, Yodoi J. Reactive oxygen-reducing and protein-refolding activities of adult T cell leukemia-derived factor/human thioredoxin. Biochem Biophys Res Commun. 1992;186:1220–1226.
6. Cronkite EP, Bullis J, Inoue T, Drew RT. Benzene inhalation produces leukemia in mice. Toxicol Appl Pharmacol. 1984;75:358–361.
7. Yoon BI, Hirabayashi Y, Kawasaki Y, et al. Mechanism of action of benzene toxicity: cell cycle suppression in hemopoietic progenitor cells (CFU-GM). Exp Hematol. 2001;29:278–285.
8. Yoshida K, Inoue T, Hirabayashi Y, Matsumura T, Nemoto K, Sado T. Radiation-induced myeloid leukemia in mice under calorie restriction. Leukemia. 1997;11(suppl 3):410–412.
9. Yoshida K, Hirabayashi Y, Watanabe F, Sado T, Inoue T. Caloric restriction prevents radiation-induced myeloid leukemia in C3H/HeMs mice and inversely increases incidence of tumor-free death: implications in changes in number of hemopoietic progenitor cells. Exp Hematol. 2006;34:274–283.
10. Till JE, McCulloch EA. A direct measurement of the radiation sensitivity of normal mouse bone marrow cells. Radiat Res. 1961;14:213–222.
11. Hirabayashi Y, Matsuda M, Aizawa S, Kodama Y, Kanno J, Inoue T. Serial transplantation of p53-deficient hemopoietic progenitor cells to assess their infinite growth potential. Exp Biol Med (Maywood). 2002;227:474–479.
12. Hirabayashi Y, Matsumura T, Matsuda M, et al. Cell kinetics of hemopoietic colony-forming units in spleen (CFU-S) in young and old mice. Mech Ageing Dev. 1998;101:221–231.
13. Yoshida K, Aizawa S, Watanabe K, Hirabayashi Y, Inoue T. Stem-cell leukemia: p53 deficiency mediated suppression of leukemic differentiation in C3H/He myeloid leukemia. Leuk Res. 2002;26:1085–1092.
14. Milner LA, Kopan R, Martin DI, Bernstein ID. A human homologue of the Drosophila developmental gene, Notch, is expressed in CD34+ hematopoietic precursors. Blood. 1994;83:2057–2062.
15. Reya T, Duncan AW, Ailles L, et al. A role for Wnt signalling in self-renewal of haematopoietic stem cells. Nature. 2003;423:409–414.
16. Bhardwaj G, Murdoch B, Wu D, et al. Sonic hedgehog induces the proliferation of primitive human hematopoietic cells via BMP regulation. Nat Immunol. 2001;2:172–180.
17. Lessard J, Sauvageau G. Bmi-1 determines the proliferative capacity of normal and leukaemic stem cells. Nature. 2003;423:255–260.
18. Sasaki H, Matsuda M, Lu Y, et al. A fraction unresponsive to growth inhibition by TGF-beta among the high-proliferative potential progenitor cells in bone marrow of p53-deficient mice. Leukemia. 1997;11:239–244.
19. Cronkite EP. Kinetics of leukemic cell proliferation. Semin Hematol. 1967;4:415–421.
20. Cronkite EP. Regulation and structure of hemopoiesis: Its application in toxicology. In: Iron RD, ed. Toxicology of the Blood and Bone Marrow. New York: Raven Press; 1985. p. 17–38.
21. Pietrzyk ME, Priestley GV, Wolf NS. Normal cycling patterns of hematopoietic stem cell subpopulations: an assay using long-term in vivo BrdU infusion. Blood. 1985;66:1460–1462.
22. Hagan M, Patchen M, Weinberg S, MacVittie T. Erythroid progenitor (BFU-E, CFU-E) proliferation as inferred from 5'bromodeoxyuridine labeling. Exp Hematol. 1994;22:1221–1226.
23. Hagan MP, MacVittie TJ. CFUs kinetics observed in vivo by bromodeoxyuridine and near-UV light treatment. Exp Hematol. 1981;9:123–128.
24. Potten CS, Chadwick C, Ijiri K, Tsubouchi S, Hanson WR. The recruitability and cell-cycle state of intestinal stem cells. Int J Cell Cloning. 1984;2:126–140.
25. Inoue T, Cronkite EP, Hirabayashi Y, Bullis JE Jr, Mitsui H, Umemura T. Lifetime treatment of mice with azidothymidine (AZT) produces myelodysplasia. Leukemia. 1997;11(suppl 3):123–127.

Hirabayashi Y, Matsuda M, Matumura T, et al. The p53-deficient hematopoietic stem cells: their resistance to radiation-apoptosis, but lasted transiently. Leukemia. 1997;11(suppl 3):489–492.
MacCay CM, Crowell MF, Maynard MF. The effect of retarded growth upon the length of the lifespan and upon the ultimate body size. J Nutr. 1935;10:63–79.
Cronkite EP, Bullis J, Inoue T, Drew RT. Benzene inhalation produces leukemia in mice. Toxicol Appl Pharmacol. 1984;75:358–361.
Delore P, Borgomano C. Leucémie aiguë au cours de l'intoxication benénique. Sur l'origine toxique de certaines leucémies aiguës et leurs relations avec less anémies graves. J de méd de Lyon. 1928;9:227–233.
30. Yoon BI, Li GX, Kitada K, et al. Mechanisms of benzene-induced hematotoxicity and leukemogenicity: cDNA microarray analyses using mouse bone marrow tissue. Environ Health Perspect. 2003;111: 1411–1420.
31. Li GX, Hirabayashi Y, Yoon BI, et al. Thioredoxin overexpression in mice, model of attenuation of oxidative stress, prevents benzene-induced hemato-lymphoid toxicity and thymic lymphoma. Exp Hematol. 2006;34:1687–1697.
32. Trosko JE, Inoue T. Oxidative stress, signal transduction, and intercellular communication in radiation carcinogenesis. Stem Cells. 1997; 15(suppl 2):59–67.

Oncogene (2007) 26, 7401–7413

www.nature.com/onc

ORIGINAL ARTICLE

Epigenetic silencing of *prostaglandin E receptor 2 (PTGER2)* is associated with progression of neuroblastomas

Y Sugino[1,2,3], A Misawa[1,2], J Inoue[1,2], M Kitagawa[4], H Hosoi[3], T Sugimoto[3], I Imoto[1,2,5] and J Inazawa[1,2,5,6]

[1]*Department of Molecular Cytogenetics, Medical Research Institute and School of Biomedical Science, Tokyo Medical and Dental University, Tokyo, Japan;* [2]*Core Research for Evolutionary Science and Technology of the Japan Science and Technology Corporation, Saitama, Japan;* [3]*Department of Pediatrics, Kyoto Prefectural University of Medicine, Kyoto, Japan;* [4]*Department of Pathology and Immunology, Graduate School, Tokyo Medical and Dental University, Tokyo, Japan;* [5]*Department of Genome Medicine, Hard Tissue Genome research Center, Graduate School, Tokyo Medical and Dental University, Tokyo, Japan and* [6]*21st Century Center of Excellence Program for Molecular Destruction and Reconstitution of Tooth and Bone, Tokyo Medical and Dental University, Tokyo, Japan*

We previously identified a cluster of prostanoid receptor genes, *prostaglandin D2 receptor* (*PTGDR*) and *prostaglandin E receptor 2* (*PTGER2*), as possible targets for DNA methylation in advanced types of neuroblastoma (NB) using bacterial artificial chromosome array-based methylated CpG island amplification method. Among them, in this study, we found that *PTGER2* was frequently silenced in NB cell lines, especially in those with *MYCN* amplification, through epigenetic mechanisms. In NB cell lines, DNA methylation pattern within a part of CpG island was inversely correlated with *PTGER2* expression, and histone H3 and H4 deacetylation and histone H3 lysine 9 methylation within the putative promoter region were more directly correlated with silencing of this gene. Methylation of *PTGER2* was observed more frequently in advanced-type of primary NBs compared with early-stage tumors. Growth of NB cells lacking endogenous PTGER2 expression was inhibited by restoration of the gene product by transient and stable transfection. A PTGER2-selective agonist, butaprost, increased intracellular cyclic adenosine monophosphate (cAMP) level, inhibited cell growth and induced apoptosis of NB cells stably expressing exogenous PTGER2. 8-Bromo-cAMP also inhibited growth of NB cells lacking PTGER2 expression, but not cells expressing this gene. Taken together, it is suggested that NB cells may lose responsiveness to PTGER2-mediated growth inhibition/apoptosis through epigenetic silencing of PTGER2 and/or disruption of downstream cAMP-dependent pathway during the neuroblastomagenesis.

Oncogene (2007) **26,** 7401–7413; doi:10.1038/sj.onc.1210550; published online 28 May 2007

Keywords: neuroblastoma; PTGER2; tumor suppressor; DNA methylation; histone modification; cAMP

Correspondence: Dr J Inazawa, Department of Molecular Cytogenetics, Medical Research Institute, Tokyo Medical and Dental University, 1-5-45 Yushima, Bunkyo-ku, Tokyo 113-8510, Japan.
E-mail: johinaz.cgen@mri.tmd.ac.jp
Received 20 February 2007; revised 23 March 2007; accepted 26 March 2007; published online 28 May 2007

Introduction

Neuroblastoma (NB) is one of the most common pediatric solid tumors of neural-crest origin. The outcome of this disease is highly heterogeneous: older patients frequently develop metastatic disease with extremely aggressive progression, whereas spontaneous regression is common in infants and in early-stage NB tumors (Westermann and Schwab, 2002; Brodeur, 2003). Although numerous genetic abnormalities, including the *MYCN* amplification, are involved in development and/or progression of NB, the molecular mechanisms responsible for the pathogenesis of aggressive NB remain unclear. Epigenetic alterations such as hypermethylation of promoter sequences, with consequent silencing of tumor-suppressor genes, such as *CASP8*, *RASSF1A*, *CD44* and *TSP-1* can play important roles in the pathogenesis of NB (Teitz *et al.*, 2000; Yan *et al.*, 2003; Yang *et al.*, 2003, 2004). Therefore, exploration of hypermethylated CpG-rich sequences in NB cell genomes could accelerate identification of unknown tumor suppressors whose loss contributes to progression of this disease.

Recently, we developed 'bacterial artificial chromosome (BAC) array-based methylated CpG-island amplification (MCA)' (BAMCA; Inazawa *et al.*, 2004), which incorporates our custom-made BAC-based genomic DNA array (Inazawa *et al.*, 2004) in combination with MCA (Toyota *et al.*, 1999), as a method for detecting aberrantly methylated sequences in the human genome. When we applied BAMCA to NB genomes using aggressive NB cell lines and stage 1 'nonaggressive' primary NB tumors as test and reference samples, respectively, followed by expression and methylation analyses of candidate targets, we successfully identified *NR1I2* as a novel tumor-suppressor candidate that is often silenced by DNA methylation in advanced type of this disease (Misawa *et al.*, 2005). In the process, we also identified several possible targets other than *NR1I2* for methylation-mediated silencing in advanced NB. Since identification of additional epigenetic abnormalities in

NB should lead not only to better understanding of the pathogenesis of this disease, but also to development of new diagnostic markers and/or therapeutic strategies (Abe *et al.*, 2005), determining the significance of each candidate tumor-suppressor gene inactivated by epigenetic mechanisms in NB will be highly valuable. Among possible targets, in the study reported here we analysed two genes, *prostaglandin E receptor 2* (*PTGER2*) and *prostaglandin D2 receptor* (*PTGDR*), both are located within the same BAC and encode receptors for subtypes of prostaglandin E2 (PGE2) and D2 respectively, and identified *PTGER2* as a candidate tumor suppressor for NB.

Results

Analysis of PTGDR *and* PTGER2 *expression in NB cell lines*

In our previous report (Misawa *et al.*, 2005), we described a strategy for identifying epigenetically silenced tumor-suppressor genes through exploration of aberrantly methylated sequences in the NB genome. During that program, *PTGDR* and *PTGER2*, within one BAC clone (RP11–262M8) at 14q22.1, were identified as possible targets for inactivation through DNA methylation (Figure 1a). To determine whether those genes might be silenced in NB, we examined expression of *PTGDR* and *PTGER2* mRNAs in a panel of 20 NB cell lines by reverse transcription (RT)–PCR. Expression of *PTGDR* was lost or decreased in most of the cell lines compared with normal adrenal gland and brain, whereas *PTGER2* expression was lost or decreased in eight lines and detected in 12 lines (Figure 1b). All eight lines that lacked expression of *PTGER2* showed amplification of *MYCN*, whereas only five of the 12 *PTGER2*-expressing lines did ($P=0.015$, Fisher's exact test).

Restoration of PTGDR *and* PTGER2 *expression by 5-aza-dCyd and TSA*

To investigate whether DNA demethylation could restore expression of *PTGDR* and *PTGER2* mRNAs in NB cells lacking them, we treated NB cells with 1 or 5 μM of 5-aza 2′-deoxycytidine (5-aza-dCyd), a methyltransferase inhibitor, for 5 days and/or 100 ng/ml of trichostatin A (TSA), a histone deacetylase inhibitor, for the last 12 h. Induction of *PTGDR* and *PTGER2* mRNAs occurred after treatment with 5-aza-dCyd in cells lacking expression of the genes (Figure 1c). Restoration of mRNA expression was also observed for both genes, especially *PTGER2*, after treatment with TSA alone. However, a greater elevation in expression was observed in cells treated with 5-aza-dCyd and TSA compared with those treated with 5-aza-dCyd alone, suggesting that DNA methylation and histone modification, including deacetylation of histones, may be cooperatively involved in silencing these two genes.

Methylation of PTGDR *and* PTGER2 *CpG islands in NB cell lines*

We examined the methylation status of CpG islands of the *PTGDR* and *PTGER2* genes predicted by the CpGPLOT program (http://www.ebi. ac.uk/emboss/cpgplot/, Figure 2a). Bisulfite-sequencing revealed aberrant DNA hypermethylation throughout the CpG island of *PTGDR* in four NB cell lines, regardless of expression levels (Figure 2b). On the other hand, aberrant DNA hypermethylation was observed within Region 3 and part of Region 2 of the *PTGER2* CpG island in three cell lines (IMR32, GOTO and SJ-N-CG) that lack expression of *PTGER2*, while this island was hypomethylated in SH-SY5Y expressing the gene. We performed combined bisulfite restriction analysis (COBRA) in a larger set of NB cell lines to confirm the relationship between expression and methylation status within the whole CpG island of *PTGDR* and within Region 3 or part of Region 3 (Region 3-A) of the *PTGER2* CpG island (Figure 2b and Supplementary Figure S1). Methylated alleles were predominant in most of the NB lines lacking *PTGER2* expression, and unmethylated alleles were always detected in cells that expressed this gene. For *PTGDR*, however, no clear relationship was observed between gene expression and methylation status of the CpG island. These results prompted us to characterize further the *PTGER2* gene as a candidate tumor suppressor inactivated through epigenetic mechanism.

Promoter activity of the CpG island of PTGER2

We performed reporter assays to determine whether the CpG island of *PTGER2*, whose methylation status was inversely correlated with gene expression, possessed promoter activity. Unexpectedly, fragment 3, where methylation was observed in NB cell lines lacking expression of *PTGER2*, revealed little promoter activity, whereas upstream fragment 1 showed remarkable activity (Figure 2c), suggesting that methylation within Region 3 of the *PTGER2* CpG island may not directly inhibit a promoter activity for gene expression, but indirectly contribute to silencing of *PTGER2* through additional epigenetic mechanisms.

Chromatin immunoprecipitation assay

Since the results of our promoter assays suggested that epigenetic mechanisms other than DNA methylation might directly regulate transcription of *PTGER2*, we postulated that histone acetylation and/or methylation might determine expression of *PTGER2* (Wolffe and Matzke, 1999; Schubeler *et al.*, 2000; Jones and Baylin, 2002; Kondo *et al.*, 2003; Nakagawachi *et al.*, 2003; Lorincz *et al.*, 2004; Stirzaker *et al.*, 2004; Strunnikova *et al.*, 2005; Azuara *et al.*, 2006; Frigola *et al.*, 2006; Yamada *et al.*, 2006), and examined status of histone modification by means of chromatin immunoprecipitation (ChIP) assays using primers designed within the putative promoter region (Figure 2a). Acetylated histone H3- and H4-binding fragments were decreased in gene-nonexpressing CHP134, SJ-N-CG and GOTO cell lines, as compared with gene-expressing SK-N-AS and SH-SY5Y cell lines

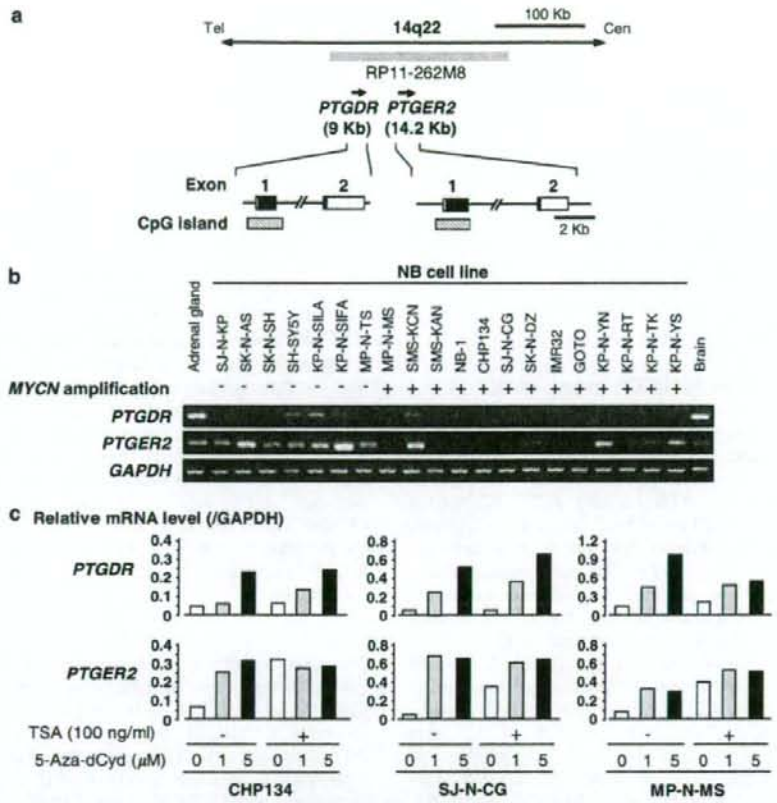

Figure 1 *PTGER2* and *PTGDR* are candidate targets for silencing in NB cells through DNA methylation. (**a**) Genomic structure of the *PTGDR* and *PTGER2* genes within the RP11–262M8 BAC clone, which was detected as one of BAC clones containing abnormally methylated sequences by BAMCA using two NB cell lines (GOTO and IMR32) as test samples and stage 1 NB tumors as control samples (Misawa *et al*., 2005). Open and filled boxes represent untranslated and coding exonic sequences respectively; hatched boxes indicate 1479 and 1482 bp CpG islands that exist around exon 1 of each gene, respectively. (**b**) RT–PCR analysis of *PTGDR* and *PTGER2* mRNAs in normal adrenal gland, normal brain and NB cell lines with (+) or without (−) amplification of *MYCN* (Saito-Ohara *et al*., 2003). Expression of *GAPDH* served as an internal control. (**c**) Representative results of RT–PCR analysis to reveal *PTGDR* and *PTGER2* mRNA expression in NB cell lines with (+) and without (−) treatment with 5-aza-dCyd and/or TSA, with *GAPDH* expression as an internal control. PCR products were electrophoresed in 3% agarose gel, and the band quantification was done with LAS-3000 (Fujifilm). Expression levels of *PTGDR* and *PTGER2* mRNA were normalized by that of *GAPDH* amplified at the same time. Experiments were repeated two times.

(Figure 2d). On the other hand, the di- and tri-methylated histone H3 lysine 9- (H3K9-) binding fragment was increased in the CHP134, SJ-N-CG and GOTO cell lines compared with SK-N-AS and SH-SY5Y cell lines (Figure 2d), suggesting that around the promoter region of *PTGER2*, histones H3 and H4 are hypoacetylated and histone H3K9 is di- and tri-methylated in NB cells lacking expression of this gene and those status of histone modification may be associated with DNA methylation within Region 3 of the *PTGER2* CpG island. This observation is consistent with the restoration of *PTGER2* expression by TSA and the observed synergistic effect of TSA together with 5-aza-dCyd (Figure 1c).

Methylation and expression of PTGER2 *in primary NB tumors*

To determine whether aberrant methylation of *PTGER2* also takes place in primary NBs, we performed methylation analyses in a panel of surgical samples using bisulfite sequencing, COBRA and methylation-specific PCR (MSP). Several stage 4 tumors showed more or less aberrant methylation within Region 3 of the *PTGER2* CpG island (Figure 3a and Supplementary Figure S1), whereas the control normal adrenal gland or stage 1 and 4S tumors did not. Using primers designed within the Region 3 (Figure 3a) based on the localization pattern of methylation, we investigated the methylation status of the Region 3 within the *PTGER2*

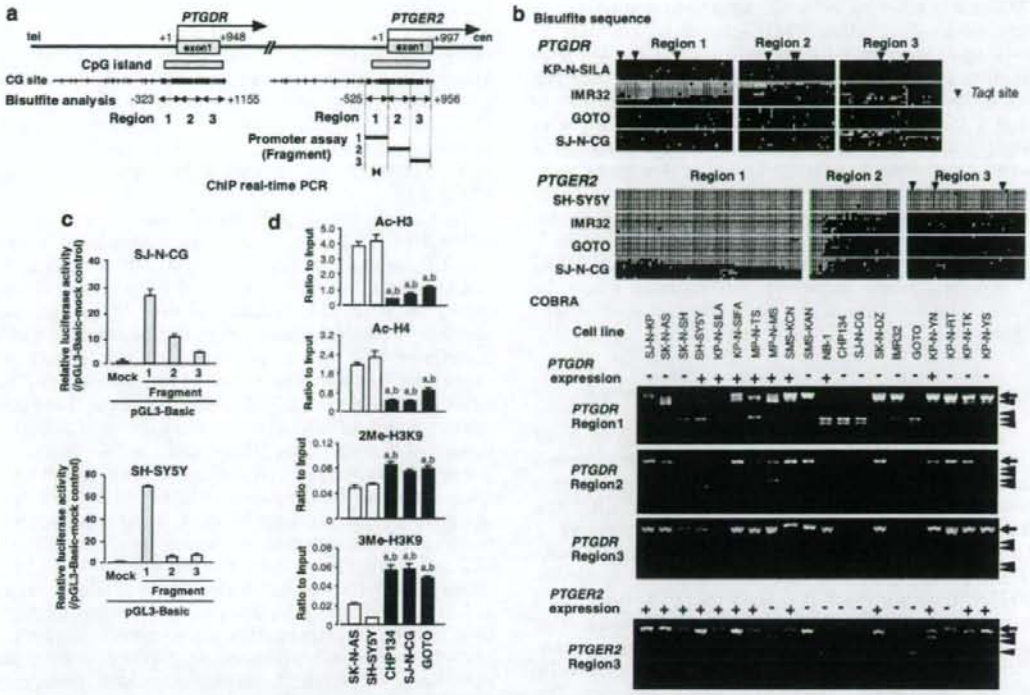

Figure 2 Association of DNA methylation and histone modification with expression status of *PTGER2*. (**a**) Map of the CpG islands (stippled bars) around the first exons of PTGDR and PTGER2. CpG sites are represented by vertical marks. Regions of each gene (Regions 1–3) examined for methylation by COBRA and bisulfite sequencing, are indicated by closed arrows. Fragments of *PTGRE2* examined in promoter assays (Fragments 1–3) are indicated by horizontal bars. The region analysed by ChIP-PCR is indicated below the map. (**b**) Left: Results of bisulfite sequencing of the CpG islands of *PTGDR* or *PTGER2* in *PTGDR* and *PTGER2* nonexpressing NB cell lines (IMR32, GOTO and SJ-N-CG) and expressing cell lines (KP-N-SILA or SH-SY5Y). Open and filled squares represent unmethylated and methylated CpG sites, respectively, and each row represents a single clone. *TaqI* restriction sites are indicated by black arrowheads. Right: Results of COBRA experiments involving Region 1–3 of the CpG island of *PTGDR* and Region 3 of the CpG island of *PTGER2* in NB cell lines with (+) or without (−) expression of each gene. PCR products were restricted by *TaqI*. Arrows indicate unmethylated alleles; arrowheads, methylated alleles. (**c**) Promoter activity of the *PTGER2* CpG island. pGL3 basic empty vectors (mock) and reporter constructs, each containing one of three different sequences within CpG island (Fragments 1–3 in Figure 2a), were transfected into a *PTGER2*-expressing cell line (SH-SY5Y) and a nonexpressing cell line (SJ-N-CG). Luciferase activities were normalized versus an internal control. The data presented are the means±s.d. of three separate experiments, each performed in triplicate. (**d**) ChIP-real time PCR assay quantitatively showing the status of histone acetylation and methylation of the *PTGER2* promoter region in NB cells *in vivo*. ChIP was performed using antibodies against acetylated histone H3 (Ac-H3), acetylated histone H4 (Ac-H4), dimethylated histone H3-lysine 9 (2Me-H3K9) and trimethylated histone H3-lysine 9 (3Me-H3K9). Experiments were performed using crosslinked extracts from PTGER2-expressing cell lines SK-N-AS and SH-SY5Y (open bars) and from PTGER2-nonexpressing cell lines CHP134, SJ-N-CG and GOTO (closed bars); immunoprecipitated samples containing the *PTGER2* promoter region were amplified by a quantitative real-time PCR (Figure 2b). A portion of the sonicated chromatin before immunoprecipitation (input) was served as a positive control for normalization, and the relative ratio to input was calculated. Differences among multiple comparisons were analysed by one-way ANOVA with subsequent Scheffé's tests: (**a**) versus SK-N-AS; (**b**) versus SH-SY5Y. All, $P<0.05$.

CpG island in all 49 surgically resected primary NBs and two ganglioneuromas. Methylation of Region 3 was detected in 12 of the 49 tumors (24.5%, Figure 3a), but not in ganglioneuromas. Of those 12 cases, four were in stage 1, 2, 3 and 4S tumors, whereas eight cases were in stage 4 ($P=0.0004$, Fisher's exact test; Figure 3b). The results of the MSP experiments were consistent with those from bisulfite sequencing (Figure 2b). Notably, eight of the nine tumors (88.9%) with *MYCN* amplification showed methylation, whereas only four of 40 tumors (10%) without amplification showed methylation ($P<0.0001$, Fisher's exact test; Figure 3b).

Expression levels of *PTGER2* mRNA in 39 primary NB tumors were evaluated by real-time quantitative RT–PCR. No significant difference was also observed between methylated and unmethylated NB cases as well as between *MYCN*-amplified and *MYCN*-unamplified NB cases ($P=0.6932$ and 0.7003, respectively, Student's *t*-test; Figure 3c). Since we conjectured that nontumorous cells such as leukocytes and endothelial cells might disturb accurate evaluation of expression levels of

PTGER2 in primary NBs, we performed immunohistochemical analysis using PTGER2-specific antibody to evaluate expression patterns in more detail. Matured ganglion cells in ganglioneuroma (Figure 3d) and NB cells differentiating to ganglion-like cells, seen mainly in stage 1 tumors with good prognosis (Figure 3e), were strongly stained with PTGER2, while the undifferentiated small round cells filling stage 4 tumors were stained weakly or not at all (Figures 3f and g). Endothelial cells and infiltrating cells, such as lymphocytes and macrophages, were also strongly stained (Figures 3f and g), suggesting that evaluation of *PTGER2* mRNA expression in whole NB samples might be affected by contamination with those normal tissue components.

Suppression of NB cell growth after restoration of PTGER2 *expression*

To gain further insight into the potential role of *PTGER2* loss in NB carcinogenesis, we investigated whether restoration of the gene product would suppress growth of NB cells lacking endogenous PTGER2. We used two kinds of PTGER2-expression constructs, a Myc-tagged full coding sequence of *PTGER2* (pcDNA-*PTGER2*-Myc) and one without epitope tag (pcDNA-*PTGER2*), with a mock construct (pcDNA-mock) as a control. Two (SJ-N-CG) or three (GOTO) weeks after transfection and subsequent selection of drug-resistant colonies, the number of large colonies produced by *PTGER2*-transfected SJ-N-CG and GOTO cells decreased markedly compared to cells containing empty vector, regardless of the existence of myc-epitope in the C-terminus (Figure 4a and Supplementary Figure S2). After transient transfection, typical apoptotic changes, such as condensation or fragmentation of nuclear chromatin, were observed more frequently in PTGER2-Myc-positive NB cells compared with either PTGER2-Myc-negative cells or control GFP-Myc-transfected cells (Figure 4b). Furthermore, stably *PTGER2*-transfected NB cells established from the SJ-N-CG and GOTO cell lines (Supplementary Figure S3a), showed a lower growth rate possibly in a PTGER2-expression level-dependent manner compared to cells transfected with control empty vector alone (mock, Figure 4c and Supplementary Figure S3b).

Effects of PGE2, butaprost and 8-Bromo-cAMP (8-Br-cAMP) on growth of NB cells

Since PTGER2 mediates a part of PGE2 signaling (Narumiya *et al*., 1999), we examined whether PGE2 would affect growth of NB cells expressing PTGER2, using stable *PTGER2* transfectants of SN-J-CG and their control counterparts (empty-vector clones). Since transfectants established from GOTO cells were not resistant to culture with serum concentrations lowered to $\leqslant 1\%$ to reduce the effect of native PGE2 in serum, only SN-J-CG transfectants were available for the experiment. In mock transfectants, as in the DLD-1 colon-cancer cell line in which butaprost promoted cell growth (Castellone *et al*., 2005), treatment with PGE2 for 72 h induced an increase in cell growth compared to treatment with vehicle alone (Figure 5a). In cells stably expressing PTGER2, on the other hand, almost no increase in cell growth was observed after treatment with PGE2 compared with vehicle alone, suggesting that growth of NB cells might be accelerated by signaling mediated through receptors for PGE2 other than PTGER2, but inhibited by signaling through PTGER2.

To confirm this hypothesis we examined growth of stable PTGER2 transfectants after treatment with a PTGER2-specific agonist, butaprost. The number of SJ-N-CG cells stably expressing PTGER2 was dramatically decreased after 72-h incubation with butaprost compared with vehicle alone, while the number of mock-transfected cells showed almost no change (Figure 5b), suggesting that signaling mediated by PTGER2, but not by other subtypes of PGE2 receptors, might specifically inhibit growth of NB cells. The same doses of butaprost promoted growth of the DLD-1 cell line. We performed fluorescence-activated cell sorting (FACS) analysis to analyse further the mechanism behind the antiproliferative effect of butaprost on NB cells. Butaprost treatment resulted in accumulation in the sub-G_1 phase of SJ-N-CG cells stably expressing PTGER2 (Figure 5c), suggesting that butaprost exerts its growth-inhibitory effect at least partly through induction of apoptosis mediated by PTGER2. Butaprost-induced apoptotic changes in SJ-N-CG cells stably expressing PTGER2 were also confirmed by terminal deoxynucleotidyl transferase (TdT)-mediated dUTP nick end-labeling (TUNEL) assay (Figure 5d). Under low-serum condition without butaprost treatment, stable PTGER2 transfectants resulted in an accumulation of cells in G_0–G_1 and a decrease in S and G_2/M phase cells compared with control counterparts (Figure 5c), suggesting that PTGER2 protein may arrest NB cells at the G_1-S checkpoint (G_0–G_1 arrest). However, no significant increase in the sub-G_1 phase was observed in stable PTGER2 transfectants compared with control counterparts (Figures 5c and d).

Since PTGER2 couples to G proteins and increases the intracellular concentration of cAMP (Narumiya *et al*., 1999), we postulated that increased intracellular cAMP might play a role in inhibiting growth of NB cells. To test this hypothesis, we examined whether stimulation of PTGER2 would induce elevation of intracellular cAMP content in stable PTGER2 transfectants of the SJ-N-CG cell line. After treatment with butaprost, a distinct increase in cAMP was observed in these transfectants, whereas no increase in cAMP occurred in mock transfectants (Figure 5b). We further examined whether increasing intracellular cAMP using a cAMP analog, 8-Br-cAMP, would mimic the effect of butaprost on growth of NB cells. Growth of GOTO and SJ-N-CG cells, which lack expression of PTGER2, was inhibited by 8-Br-cAMP, whereas growth of SJ-N-KP and KP-N-SIFA, which express PTGER2, showed almost no change (Figure 6a). FACS analysis showed accumulation of GOTO and SJ-N-CG cells in the sub-G_1 phase after treatment with 8-Br-cAMP (Figure 6a).

Discussion

In a previous study (Misawa *et al*., 2005), we identified the *PTGDR* and *PTGER2* genes as possible targets for DNA methylation in advanced types of NB. In the work presented here, we have demonstrated that expression of *PTGER2* was often silenced in NB cell lines through epigenetic mechanisms such as DNA methylation and

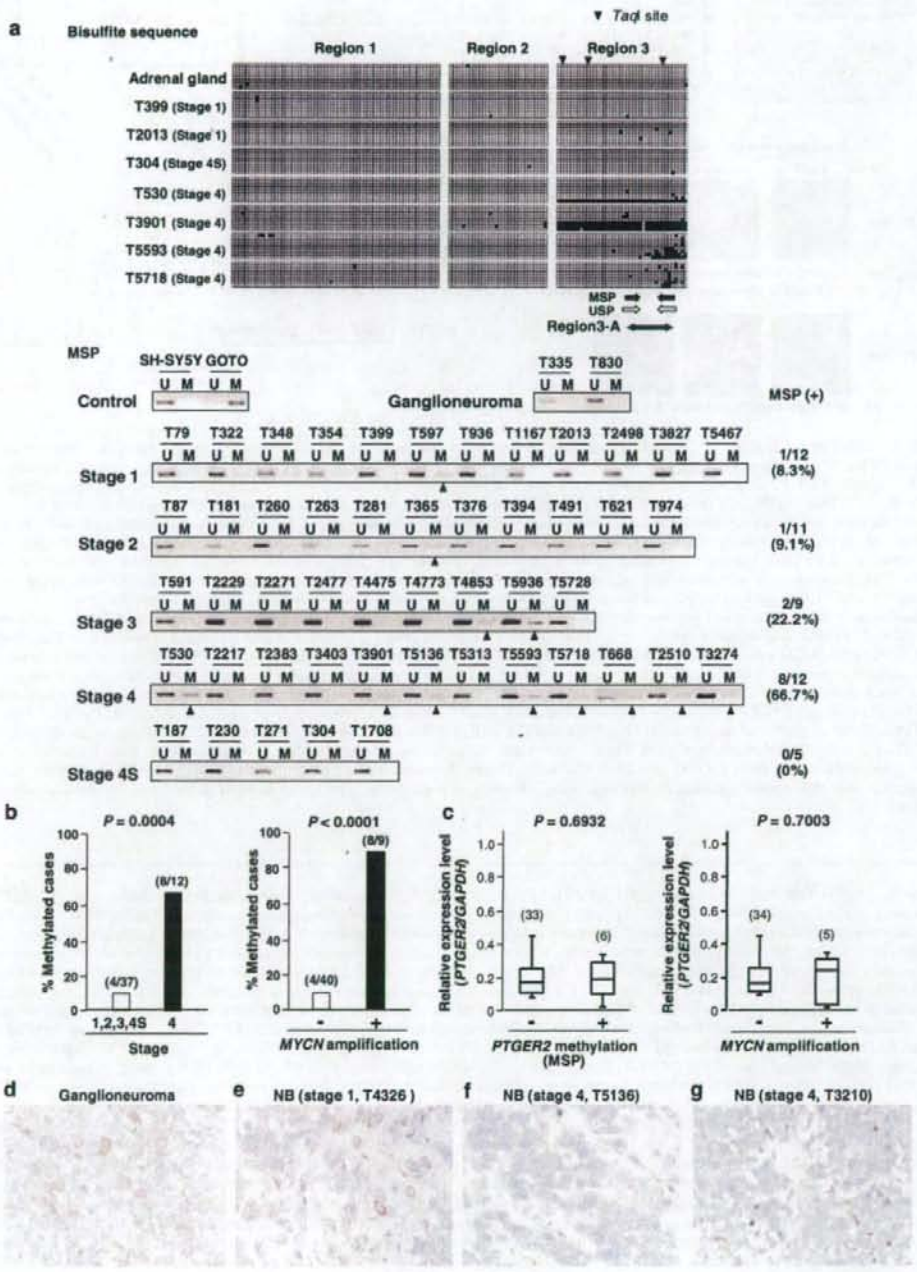

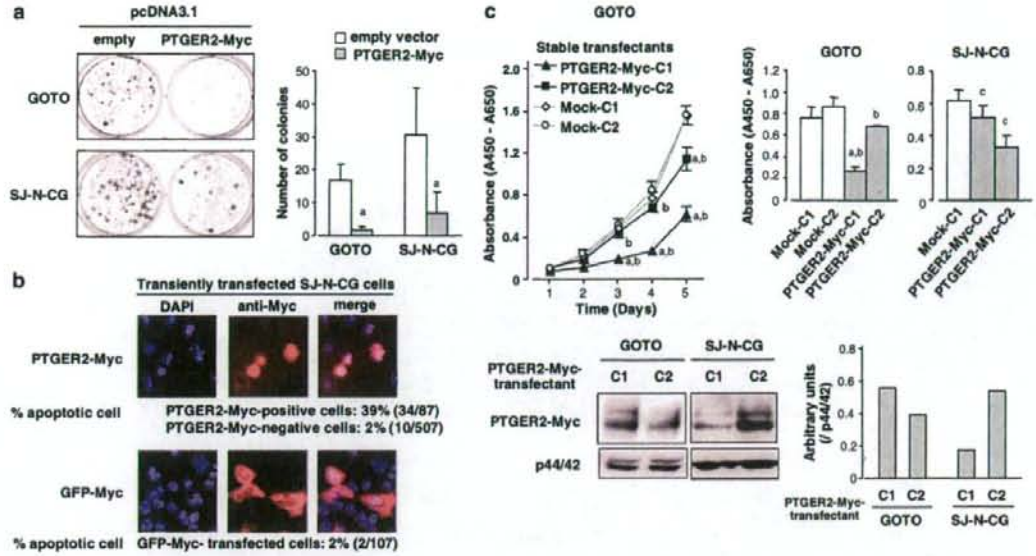

Figure 4 Effect of restoration of *PTGER2* expression on growth of NB cells. (**a**) Colony-formation assays using two NB cell lines without *PTGER2* expression (GOTO and SJ-N-CG). The cells were transiently transfected with a Myc-tagged construct containing *PTGER2* (pcDNA3.1-*PTGER2*-Myc), or empty vector (pcDNA3.1-empty) and selected for 2–3 weeks with appropriate concentrations of G418. Left: Two (SJ-N-CG) or three (GOTO) weeks after transfection and subsequent selection of drug-resistant colonies, the colonies formed by *PTGER2*-transfected cells were less numerous than those formed by empty vector-transfected cells. Right, Quantitative analysis of colony formation. Colonies larger than 2 mm were counted, and results are presented as means ± s.d. of representative of three separate experiments, each performed in triplicate. Statistical analysis used the Mann–Whitney *U*-test: (**a**) $P<0.05$ versus empty vector-transfected cells. (**b**) Fluorescent immunocytochemical analysis of SJ-N-CG cells transiently transfected with Myc-tagged *PTGER2* and stained with anti-Myc-tag antibody. Notably, cells with typical apoptotic changes, such as condensation or fragmentation of nuclear chromatin, were observed more frequently in PTGER2-Myc-positive NB cells compared with either PTGER2-Myc-negative cells or control GFP-Myc-transfected cells. (**c**) Effect of stable PTGER2 expression on the growth of GOTO and SJ-N-CG cells. Viability was determined by WST assay at the indicated times. The data presented are the means ± s.d. of three separate experiments. Statistical analysis used one-way ANOVA with subsequent Scheffé's tests: (**a**) PTGER2-transfected clone versus mock control clone C1 established from GOTO cells; (**b**) PTGER2-transfected clone versus mock control clone C2 established from GOTO cells; (**c**) PTGER2-transfected clone versus mock control clone C1 established from SJ-N-CG cells. All, $P< 0.05$. Upper left: Time course of growth of stably mock- (mock-C1 and C2) or PTGER2- (PTGER2-Myc-C1 and C2) transfected clones established from GOTO cells (Supplementary Figure S3a). Upper right: Comparison of the number of viable cells at day 4 among stable transfectants established from GOTO and SJ-N-CG cells. Lower: Expression level of transfected PTGER2 protein in each stable transfectant was determined by western blotting using anti-Myc-tag antibody. The quantification determined by densitometer is provided.

Figure 3 Methylation and expression status of *PTGER2* in primary NB tumors. (**a**) Upper, Representative results of bisulfite sequencing of the CpG islands of *PTGER2* in primary NB tumors and the normal adrenal gland as a control. See legend for Figure 2b for interpretation. Black (MSP) and white (USP) arrows indicate the positions of primer sequences designed to amplify methylated and unmethylated alleles, respectively, in MSP experiments. Closed arrow (Region 3-A) indicates commonly methylated region in cell lines and primary tumors of NB (Supplementary Figure S1). Lower, Results of MSP experiments for 49 primary NB tumors and two ganglioneuromas. DNAs from SH-SY5Y and GOTO cell lines were used for unmethylated and methylated controls, respectively. Arrowheads indicate methylated alleles. (**b**) *PTGER2* methylation status of primary NB tumors, compared with tumor stage (left) and *MYCN* amplification status (right). Methylation status was determined by MSP. Left: The *PTGER2* CpG island was methylated in four of 37 stage 1, 2, 3 or 4S tumors (10.8%), while 8 of 12 (66.7%) stage 4 tumors showed methylated alleles ($P=0.0004$, Fisher's exact test). Right: Methylation of the *PTGER2* CpG island in eight of the nine tumors (88.9%) with *MYCN* amplification; only four of 40 (10%) tumors without *MYCN* amplification show methylated alleles ($P<0.0001$, Fisher's exact test). (**c**) Expression of *PTGER2* mRNA in 39 primary NB tumors, compared with methylation status of the *PTGER2* Region 3 (left) and *MYCN* amplification status (right). The levels of *PTGER2* mRNA expression were determined by real-time quantitative RT–PCR experiments. Median values are indicated with horizontal bars in the boxes. The vertical bars indicate the range and the horizontal boundaries of the boxes represent the first and third quartiles. The number of cases in each group is in parentheses. Statistical analysis used the Student's *t*-test. The number of cases in each group is in parentheses. (**d–g**) Representative immunohistochemical analysis of PTGER2 protein using specific antibody. (**d**) Ganglioneuroma. Matured ganglion cells showed strong PTGER2 immunoreactivity. (**e**) Stage 1 tumors of NB with good prognosis. NB cells differentiating to ganglion-like cells showed strongly PTGER2 immunoreactivity, whereas undifferentiated small round cells showed weak PTGER2 immunoreactivity. (**f** and **g**) Stage 4 NB tumors with *MYCN* amplification. Undifferentiated small round cells showed very weak or no PTGER2 immunoreactivity. Note that nontumorous mesenchymal cells, including endothelial cells and infiltrating cells such as lymphocytes and macrophages, were strongly stained for PTGER2.

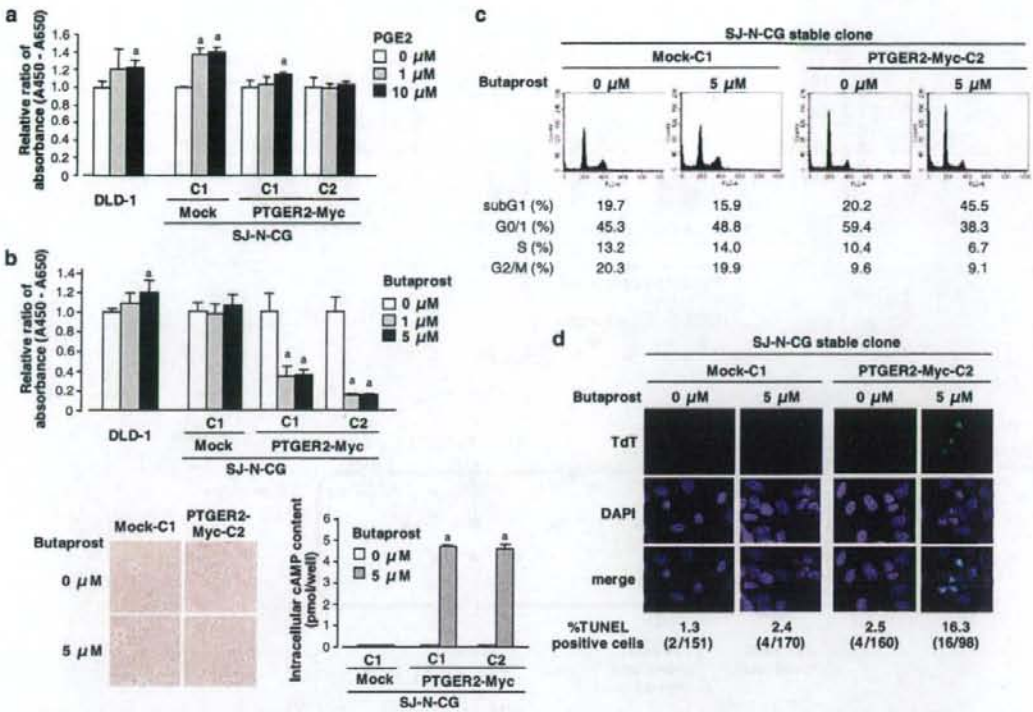

Figure 5 Inhibition of NB cell growth by PTGER2-mediated signaling. (**a**) Effect of PGE2 on growth of NB cells stably expressing PTGER2. After preculture for 24 h in medium containing 1% FBS, stable mock (mock-C1) or PTGER2 (PTGER2-Myc-C1 and C2) transfectants established from SJ-N-CG cells were treated with 0, 1, or 10 μM of PGE2 for 3 days and cell viability was determined by WST assay. The effect of PGE2 on cell growth was shown by absorbance of PGE2-treated cells relative to that of vehicle-treated cells (relative ratio). Statistical analysis used one-way ANOVA with subsequent Scheffé's tests: (**a**) $P<0.05$ versus cells treated with vehicle alone. Note that DLD-1, a colorectal-cancer cell line whose growth is promoted by PGE2 through a PTGER2-mediated signaling pathway other than a cAMP-dependent one, showed an increase in cell numbers after treatment with PGE2 for 72 h. (**b**) Effect of a specific PTGER2 agonist, butaprost, on growth and levels of intracellular cAMP in NB cells stably expressing PTGER2. Left, after preculture for 24 h in medium containing 1% FBS, stable mock (mock-C1) or PTGER2 (PTGER2-Myc-C1 and C2) transfectants established from SJ-N-CG cells were treated with 0, 1, or 5 μM of butaprost for 3 days and cell viability was determined by WST assay. The effect of butaprost on cell growth is shown as a relative ratio, as described in (**a**). Statistical analysis used one-way ANOVA with subsequent Scheffé's tests: (**a**) $P<0.05$ versus cells treated with vehicle alone. Note that DLD-1 showed an increase in cell numbers after treatment with butaprost for 72 h. Right: after 24-h preculture in medium containing 1% FBS, stable mock (mock-C1) or PTGER2 (PTGER2-Myc-C1 and C2) transfectants established from SJ-N-CG cells were treated with 0 or 5 μM of butaprost for 20 min. Levels of intracellular cAMP were determined by a cAMP EIA system (GE Healthcare Bio-Sciences, Piscataway, NJ, USA) according to the manufacturer's protocol. Statistical analysis used the Mann–Whitney *U*-test; (**a**) $P<0.05$ versus vehicle-treated control cells. (**c**) FACS analysis of PTGER2-stable transfectant (PTGER2-Myc-C2) and control clones (mock-C2). PTGER2-stable transfectants established from SJ-N-CG cells accumulated in G_0–G_1 phase in comparison with control clones. Notably, an increase in the sub-G_1 fraction and a decrease in the G_2/M fraction were observed in butaprost-treated PTGER2 transfectants. (**d**) Representative image of TUNEL staining in stable mock (mock-C1) and PTGER2 (PTGER2-Myc-C2) transfectants of SJ-N-CG with or without butaprost treatment. More TUNEL-positive cells were detected in stable PTGER2 transfectants treated with 5 μM of butaprost (16.3%) than in transfectants treated with vehicle alone (2.5%); the number of TUNEL-positive cells in mock-transfectant cultures was not affected by butaprost. Magnifications are $\times 400$.

histone modification, especially in *MYCN*-amplified cells. Methylation of *PTGER2* was also observed in advanced primary NB tumors, although its direct correlation with expression status in primary NBs remains unclear due to high expression levels of *PTGER2* in unavoidable nontumor cells. Growth of NB cell lines lacking expression of *PTGER2* was inhibited by exogenous restoration of the gene product. Moreover, a PTGER2-specific agonist inhibited growth of transfected NB cell lines that were stably expressing exogenous PTGER2, at least in part through production of cAMP as a second messenger in those cells.

PTGER2 locates in 14q22.1, a chromosomal region that is involved in loss of heterozygosity (LOH) or copy-number losses in 20–25% of NBs, although the smallest region of overlapping LOH at 14q is more distal (14q23-qter; Thompson *et al*., 2001). Indeed, most of the cell lines we used in this study showed normal copy numbers

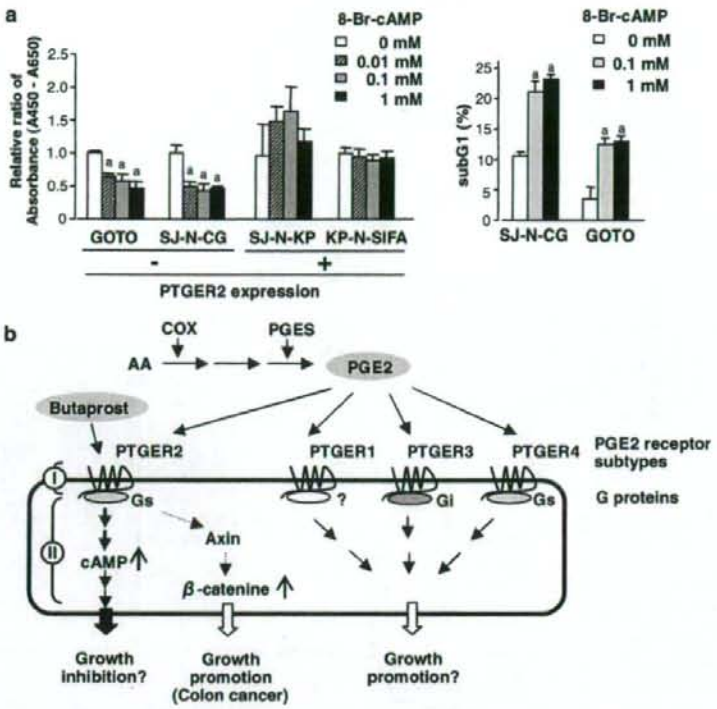

Figure 6 (**a**) Left: Effect of a cell-permeable cAMP analog, 8-Br-cAMP, on growth of NB cells. Wild-type GOTO and SJ-N-CG cells, which lack expression of *PTGER2*, and SJ-N-KP and KP-N-SIFA, which do express the gene, were cultured for 72 h with various concentrations of 8-Br-cAMP or no 8-Br-cAMP, and cell viability was determined by WST assay. The effect of 8-Br-cAMP on cell growth is shown as a relative ratio, as described for (**a**). Statistical analysis used one-way ANOVA with subsequent Scheffé's tests: (**a**) $P<0.05$ versus cells treated with vehicle alone. Notably, 8-Br-cAMP inhibited cell growth in GOTO and SJ-N-CG cells, but not in SJ-N-KP and KP-N-SIFA. Right: An increase in sub-G_1 fraction was observed after treatment with 8-Br-cAMP in GOTO and SJ-N-CG cells. Wild-type GOTO and SJ-N-CG cells, which lack expression of *PTGER2*, were cultured with 0, 0.1, or 1.0 mM of 8-Br-cAMP for 72 h. The data presented are the means ± s.d. of three separate experiments. Statistical analysis used one-way ANOVA with subsequent Scheffé's tests: (**a**) $P<0.05$ versus 0 mM of 8-Br-cAMP treated cells. (**b**) Schematic representation of interactions among PTGER2 signals and cell growth. COX, cyclo-oxygenase; PGES, prostaglandin E synthase. The PTGRE2 signaling pathway may be disrupted in NB cells through epigenetic silencing of *PTGRE2* (I). Alternatively or in addition, disruption of downstream signaling, including unresponsiveness to cAMP (II), may contribute to loss of the tumor-suppressive activity of normal PGE2-PTGRE2 signaling.

at 14q22 in conventional (Saito-Ohara *et al*., 2003) and BAC array-based (unpublished data) comparative genomic hybridization (CGH) experiments, suggesting that homozygous inactivation of *PTGER2* might occur through biallelic DNA methylation/histone modification in NB cells.

The putative 'core promoter region' of *PTGER2*, which showed high promoter activity in our reporter assay, was not methylated in some of the NB cell lines we analysed regardless of the gene's expression status, although aberrant DNA methylation in exonic region (Region 3) of *PTGER2* was inversely correlated with expression in NB cell lines. On the other hand, within the putative 'core promoter region' the acetylation status of H3 and H4 histones, and the di- and trimethylation status of H3K9, were positively and inversely correlated with *PTGER2* expression, respectively. In view of these observations, we speculate that silencing of *PTGER2* in NB cells depends on integrated epigenetic events such as DNA methylation and histone modification. This phenomenon has been observed in other genes, including tumor-suppressor genes among a variety of solid tumors (Nakagawachi *et al*., 2003; Stirzaker *et al*., 2004; Strunnikova *et al*., 2005; Frigola *et al*., 2006; Yamada *et al*., 2006).

Epigenetic mechanisms of tumor-suppressor-gene silencing in cancer remains incompletely understood (Jones and Baylin, 2002). It is believed that DNA sequences in entire CpG islands with promoter activity are methylated, H3 and H4 are unacetylated and H3K9 is methylated. However, it was also reported that hypermethylation of nonpromoter exonic sequences affects heterochromatinization and local gene silencing (Frigola *et al*., 2006). In some cancer-associated gene silencing, moreover, sequences outside the promoter region may be methylated first (Jones and Baylin, 2002;

Nakagawachi *et al.*, 2003; Stirzaker *et al.*, 2004; Strunnikova *et al.*, 2005;), and this methylation could induce histone modifications such as deacetylation of lysine residues by histone deacetylase and H3K9 di- and tri-methylation by histone methyltransferase (Kondo *et al.*, 2003; Stirzaker *et al.*, 2004; Strunnikova *et al.*, 2005), mediated by methyl-CpG-binding proteins. These processes lead to condensation of the chromatin, which propagates into a transcription factor-binding region, making target sequences inaccessible to transcription factors; finally gene transcription is shut off (Jones and Baylin, 2002; Nakagawachi *et al.*, 2003). Consequently, methylation outside the promoter region could lead gene silencing indirectly, although histone modification within the critical promoter region may contribute to silencing directly. This scenario is consistent with our results showing that TSA alone can partially restore expression of *PTGER2* and that TSA and 5-aza-dCyd exert a synergistic effect on restoring expression of this gene.

Using primary NB tumors, we showed that *PTGER2* methylation within Region 3 occured more frequently in aggressive NBs such as stage 4 tumors than early-stage tumors, and in tumors with *MYCN* amplification than tumors without its amplification. Therefore the methylation status of this gene might be useful for predicting the aggressiveness of NB tumors, although our set of tumors was not suitable for survival analysis because few of the patients died during the follow-up period. Since PTGER2 is expressed in nontumorous cells, such as endothelial cells, and also in infiltrating lymphocytes and macrophages, it will be difficult to evaluate correlation between silenced *PTGER2* expression and methylation status of NB cells in clinical samples. To clarify the clinical significance of the *PTGER2* gene in NB, further examination of methylation status, not expression status, of this gene in a larger set of primary cases of NB will be required.

One of the most striking findings in the study reported here is that restoration of PTGER2 protein by either transient or stable transfection of expression constructs inhibited growth of NB cells that lacked endogenous *PTGER2*. Moreover, a PTGER2-specific agonist (butaprost) inhibited growth of NB cells stably expressing exogenous PTGER2, at least partly by inducing apoptosis. Those results suggested that negative regulation of cell growth, including induction of apoptosis, was a significant consequence of ectopic expression of PTGER2 in NB cells lacking expression of this gene.

PGE2 is biosynthesized from arachidonic acid as a major cyclo-oxygenase product in a number of physiological settings, and produces a broad range of biologic actions in diverse tissues (Narumiya *et al.*, 1999). It was shown that cyclo-oxygenase-2 (COX-2) is expressed in NB, and COX-inhibiting nonsteroidal anti-inflammatory drugs inhibit growth of NB cells *in vitro* and *in vivo* (Johnsen *et al.*, 2004). In some tumors, including colon cancer, PGE2 has been implicated in promotion of tumor growth, promotion of angiogenesis, inhibition of apoptosis, stimulation of invasion, or suppression of immune responses (Hoshino *et al.*, 2003; Hata and Breyer, 2004; Castellone *et al.*, 2005; Wang *et al.*, 2005a, 2006; Wang and DuBois, 2006). Those activities indicate that genes encoding receptors for PGE2 and/or its downstream targets can act as oncogenes. However, PGE2 can also act anti-proliferatively in some tumors, inducing apoptosis or differentiation (Santoro *et al.*, 1977; Fulton *et al.*, 1989; Fedyk *et al.*, 1996; Okuyama *et al.*, 2002), indicating that receptors for PGE2 and/or its downstream targets also can function as tumor suppressors.

Signaling of PGE2 is mediated by four receptors (PTGRE 1–4); the physiological/pathophysiological behavior of PGE2 appears to depend on the type of its receptors and on downstream pathways, accounting for completely opposite effects (Narumiya *et al.*, 1999). Although an antiapoptotic effect of PTGER2 in gastric mucosal cells (Hoshino *et al.*, 2003) and a growth-promoting effect in colon-cancers via the PTGER2-G_s-axin-β-catenin signaling pathway (Castellone *et al.*, 2005) have been reported, several lines of evidence show that PTGER2 also can negatively regulate cell growth and induce apoptosis and/or differentiation in various types of cells (Fedyk *et al.*, 1996; Suda *et al.*, 1996; Okuyama *et al.*, 2002). Thus, the role played by the PGE2-PTGER2 signaling pathway may vary considerably from one neoplasm to another, probably in a tissue- or cell lineage-dependent manner. This hypothesis is consistent with our results demonstrating that butaprost promoted cell growth in colon-cancer cell line DLD-1, as expected on the basis of published data (Castellone *et al.*, 2005), but inhibited growth of NB cells stably expressing PTGER2. In NB, disruption of the PTGER2-mediated growth-suppressive pathway may contribute to tumor progression.

The question of how the cellular context is able to determine the action of PGE2-PTGER2 signaling in NB cells is extremely interesting and deserves further investigation. PGE2 increases intracellular concentrations of cAMP through PTGER2 and PTGER4 and some splice variants of PTGER3, coupling to G proteins (Narumiya *et al.*, 1999). Among PGE2 receptors, PTGER2 has the most potential for elevating intracellular cAMP concentrations (Regan, 2003). Since elevated levels of cAMP are associated with decreased proliferation and increased differentiation or apoptosis in several types of cells including glioblastoma cells (Chen *et al.*, 1998), esophageal squamous cell carcinomas (Wang *et al.*, 2005b), and hippocampal cells (Takadera *et al.*, 2004), we speculate that PTGER2-mediated production of intracellular cAMP may contribute to the growth-inhibitory effect of restored PTGER2 in NB cells lacking endogenous expression of the gene. In our experiments a PTGER2-specific agonist increased intracellular cAMP levels and exerted growth inhibitory effects, at least partly by inducing apoptosis, in stable PTGER2 transfectants established from the SJ-N-CG cell line, although G_0–G_1 arrest but not apoptosis was predominantly observed in PTGER2 transfectants under low-serum condition without butaprost treatment. A similar effect of butaprost in hippocampal cells has been reported (Takadera *et al.*,

2004), even though those cells were nontumorous. The fact that a cAMP analog, 8-Br-cAMP, which directly increases intracellular cAMP, inhibited cell growth and induced apoptosis in NB cells lacking endogenous PTGER2, but not in those expressing PTGER2, suggested that NB cells may lose responsiveness to PTGER2-mediated growth inhibition/apoptosis through epigenetic silencing of PTGER2 (I in Figure 6b) or by disruption of a downstream cAMP-dependent signaling pathway (II in Figure 6b). Further examination will be needed to clarify the biological and clinical significance of the PGE2-PTGER2-cAMP signaling pathway in the pathogenesis of NB, especially with regard to the resistance of advanced NB tumors to apoptosis (del Carmen Mejia *et al*., 2002).

Materials and methods

Cell culture and primary tissue samples

All 20 human NB cell lines we used (SJ-N-KP, SK-N-AS, SK-N-SH, SH-SY5Y, KP-N-SILA, KP-N-SIFA, MP-N-TS, MP-N-MS, SMS-KCN, SMS-KAN, NB-1, CHP134, SJ-N-CG, SK-N-DZ, IMR32, GOTO, KP-N-YN, KP-N-RT, KP-N-TK, KP-N-YS) had been established from surgically resected tumors (Saito-Ohara *et al*., 2003). The DLD-1 colon-cancer cell line was purchased from the Japanese Collection of Research Bioresources (Osaka, Japan). Cells were maintained in RPMI-1640, supplemented with 10% fetal bovine serum (FBS) and 100 U/ml penicillin/100 μg/ml streptomycin. NB cells were treated with or without 1 or 5 μM of 5-aza-dCyd for 5 days, and/or 100 ng/ml of TSA for the last 12 h.

Primary tumor samples were obtained at surgery from 49 patients with NB and two with ganglioneuroma who underwent tumor resection at University Hospital, Kyoto Prefectural University of Medicine from 1986 to 2003, with written consent from the parents of each patient in the formal style and after approval by the local ethics committees. Staging of each NB case was determined according to the criteria of the International Neuroblastoma Staging System (Brodeur *et al*., 1993). Of the 49 NB patients, 41 (83.7%) were infants less than 18 months of age at diagnosis, 36 (73.5%) were detected by a mass-screening program, 12 were classified as stage 1, 11 as stage 2, nine as stage 3, 12 as stage 4 and five as stage 4S; *MYCN* amplification was detected in the tumors of nine (18.4%) patients. Genomic DNA was available for analysis from all 49 NB and two ganglioneuroma samples; total RNA was available from 39 NB samples.

Reagents and plasmids

PGE2, butaprost and 8-Br-cAMP were obtained respectively from Calbiochem (San Diego, CA, USA), Cayman Chemicals (Ann Arbor, MI, USA) and Sigma-Aldrich (St Louis, MO, USA). Anti-PTGER2 polyclonal antibody was from Cayman Chemicals. Anti-acetylated histone H3 (anti-AcH3), anti-acetylated histone H4 (anti-AcH4), anti-dimethylated histone H3 lysine 9 (anti-2Me-H3K9) and anti-trimethylated histone H3 lysine 9 (anti-3Me-H3K9) antibodies were from Upstate (Lake Placid, NY, USA); anti-Myc-tag and anti-p44/42 antibodies were from Cell Signaling Technology (Beverly, MA, USA).

Plasmids expressing PTGER2 alone (pcDNA3.1-*PTGER2*) C-terminally Myc-tagged PTGER2 (pcDNA3.1-*PTGER2*-Myc) were prepared by cloning the RT–PCR product of the full coding sequence of *PTGER2* alone, or in-frame along with the Myc-epitope in the C terminus, respectively, into the vector pcDNA3.1 (Invitrogen, Carlsbad, CA, USA). The empty vector pcDNA3.1 or plasmid expressing Myc-tagged GFP (pcDNA3.1-GFP-Myc) was used as a control.

RT–PCR and real-time quantitative RT–PCR

Single-stranded cDNAs generated from total RNAs were amplified with primers specific for each gene (Supplementary Table S1). The glyceraldehyde-3-phosphate dehydrogenase gene (*GAPDH*) was amplified at the same time to allow estimation of the efficiency of cDNA synthesis. RT–PCR products were electrophoresed, and quantified with LAS-3000 (Fujifilm, Tokyo, Japan). Levels of mRNA expression in primary tumors were measured using a quantitative real-time fluorescence detection method (PRISM 7900HT, Applied Biosystems, Foster City, CA, USA) according to the manufacturer's protocol. The expression of *PTGER2* mRNA in each sample was normalized on the basis of the respective *GAPDH* content and recorded as a relative expression level. PCR amplification was performed in duplicate for each sample.

Methylation analysis

Genomic DNAs were treated with sodium bisulfite, and subjected to PCR using primer sets designed to amplify regions of interest (Supplementary Table S1). For COBRA, PCR products were digested with *Taq*I, and electrophoresed (Xiong and Laird, 1997). For bisulfite sequencing, the PCR products were subcloned and then sequenced.

For MSP, sodium bisulfite-treated DNA was amplified using primers specific to the methylated and unmethylated forms of DNA sequences (Supplementary Table S1). DNAs from cell lines recognized as unmethylated or highly methylated by bisulfite sequencing were used as controls.

Promoter assay

DNA fragments around the CpG-island predicted by the CpGPLOT program (http://www.ebi.ac.uk/emboss/cpgplot/) were ligated into the vector pGL3-Basic (Promega, Madison, WI, USA). Promoter assay using each construct or control vector with an internal control vector (pRL-hTK, Promega) was performed as described elsewhere (Misawa *et al*., 2005).

ChIP assay

ChIP assays were performed as described previously (Sonoda *et al*., 2004). Chromatin was immunoprecipitated with anti-AcH3, anti-AcH4, anti-2Me-H3K9, anti-3Me-H3K9, or no antibody, after which a quantitative real-time PCR was performed with 1/30 of the immunoprecipitated DNA, using primers designed to amplify regions of interest (Supplementary Table S1); 1/600 of the solution before adding antibody was amplified as an internal control for the amount of DNA.

Immunohistochemistry

Formalin-fixed, paraffin-embedded surgical specimens were sliced into 5 μm-thick sections, deparaffinized, then immersed for 30 min in methanol containing 0.3%. hydrogen peroxide. After retrieval of epitope by boiling, the sections were incubated with anti-PTGER2 antibody (1:500 dilution) and then with a biotinylated secondary antibody (1:200 dilution; Vector Laboratories, Burlingame, CA, USA). After staining with Vectastain ABC reagent (Vector Laboratories), the sections were immersed in 0.05% diaminobenzidine tetrahydrochloride solution containing 0.01% hydrogen peroxide, and counterstained with hematoxylin.

Transient transfection and colony-formation assays
pcDNA3.1-*PTGER2*, pcDNA3.1-*PTGER2*-Myc or the empty-vector (pcDNA3.1-mock) were transiently transfected into SJ-N-CG and GOTO cells using FuGENE6 (Roche Diagnostics, Tokyo, Japan) for colony-formation assays. Expression of PTGER2 protein in transfected cells was confirmed by western blotting, using anti-Myc-Tag or anti-PTGER2 antibody as described elsewhere (Misawa *et al*., 2005). After 2–3 weeks of incubation with G418 (600 and 250 μg/ml for SJ-N-CG and GOTO, respectively), cells were stained with crystal violet.

Immunofluorescent staining
Transiently or stably transfected cells seeded into slide chambers were fixed in cold methanol for 3 min. The cells were covered with blocking solution (1% skim milk in phosphate-buffered saline) for 30 min, and incubated overnight at 4°C with anti-Myc-tag antibody (1:200 dilution) in blocking solution. There followed 1 h of incubation with Alexa 594-conjugated goat anti-mouse IgG (1:500 dilution; Molecular Probes, Eugene, OR, USA). The cells were counterstained with 4′,6-diamidino-2-phenylindole, and viewed with an ECLIPSE E800 fluorescence microscope (Nikon, Tokyo, Japan).

Establishment of stable transfectants and cell-growth assay
Stable transfectants of *PTGER2* and mock vector were obtained by transfecting pcDNA3.1-*PTGER2*-Myc. and pcDNA3.1-mock, respectively, into SJ-N-CG and GOTO cells, and selected by G418. For measurements of cell growth, 2×10^3 cells were seeded in 96-well plates. To determine the effects of PGE2, butaprost, or 8-Br-cAMP on growth of NB cells, wild type cell lines or stable transfectants of SJ-N-CG cells were treated with various concentrations of each reagent for 72 h, after 24-h preculture in media containing 1% FBS (for PGE2 and butaprost) or 10% FBS (for 8-Br-cAMP). The numbers of viable cells were assessed by a colorimetric water-soluble tetrazolium salt (WST) assay as described elsewhere (Misawa *et al*., 2005). The DLD-1 cell line was served as a positive control for the PGE2 and butaprost experiments (Castellone *et al*., 2005).

Enzyme immunoassay
After 24-h pre-culture in medium containing 1% FBS, stable transfectants of SJ-N-CG cells were treated with 0 or 5 μM of butaprost for 20 min. Intracellular cAMP was measured by means of a cAMP Enzyme immunoassay (EIA) system (GE Healthcare Bio-Sciences, Piscataway, NJ, USA) according to the manufacturer's protocol.

Flow cytometry
Stable transfectants of SJ-N-CG cells were treated with butaprost (5 μM) or 8-Br-cAMP (0.1 or 1 mM) for 72 h. For FACS analysis, harvested cells were fixed in 70% cold ethanol before treatment with RNaseA and propidium iodide. Samples were analysed on a FACSCalibur HG (Becton-Dickinson, San Jose, CA, USA). Data were analysed using BD CellQuest Pro (Becton-Dickinson).

TUNEL stain
Wild-type or stable transfectants of SJ-N-CG cells were treated with or without butaprost or 8-Br-cAMP, and apoptosis was detected by enzymatic labeling of DNA strand-breaks using a TUNEL staining kit (MEBSTAIN Apoptosis Kit Direct; MBL, Aichi, Japan) according to the manufacturer's protocol.

Acknowledgements

This work was supported by Grants-in-Aid for Scientific Research on Priority Areas (C) from the Ministry of Education, Culture, Sports, Science and Technology, Japan; by a Grant-in-Aid from Core Research for Evolutional Science and Technology (CREST) of the Japan Science and Technology Corporation (JST); and by a 21st Century Center of Excellence (COE) Program for Molecular Destruction and Reconstitution of Tooth and Bone.

References

Abe M, Ohira M, Kaneda A, Yagi Y, Yamamoto S, Kitano Y *et al*. (2005). CpG island methylator phenotype is a strong determinant of poor prognosis in neuroblastomas. *Cancer Res* **65**: 828–834.

Azuara V, Perry P, Sauer S, Spivakov M, Jorgensen HF, John RM *et al*. (2006). Chromatin signatures of pluripotent cell lines. *Nat Cell Biol* **8**: 532–538.

Brodeur GM, Pritchard J, Berthold F, Carlsen NL, Castel V, Castelberry RP *et al*. (1993). Revision of the international criteria for neuroblastoma diagnosis, staging, and response to treatment. *J Clin Oncol* **11**: 1466–1477.

Brodeur GM. (2003). Neuroblastoma: biological insights into a clinical enigma. *Nat Rev Cancer* **3**: 203–216.

Castellone MD, Teramoto H, Williams BO, Druey KM, Gutkind JS. (2005). Prostaglandin E2 promotes colon cancer cell growth through a GS-axin-beta-catenin signaling axis. *Science* **310**: 1504–1510.

Chen TC, Hinton DR, Zidovetzki R, Hofman FM. (1998). Up-regulation of the cAMP/PKA pathway inhibits proliferation, induces differentiation, and leads to apoptosis in malignant gliomas. *Lab Invest* **78**: 165–174.

del Carmen Mejia M, Navarro S, Pellin A, Ruiz A, Castel V, Llombart-Bosch A. (2002). Study of proliferation and apoptosis in neuroblastoma. Their relation with other prognostic factors. *Arch Med Res* **33**: 466–472.

Fedyk ER, Ripper JM, Brown DM, Phipps RP. (1996). A molecular analysis of PGE receptor (EP) expression on normal and transformed B lymphocytes: coexpression of EP1, EP2, EP3beta and EP4. *Mol Immunol* **33**: 33–45.

Frigola J, Song J, Stirzaker C, Hinshelwood RA, Peinado MA, Clark SJ. (2006). Epigenetic remodeling in colorectal cancer results in coordinate gene suppression across an entire chromosome band. *Nat Genet* **38**: 540–549.

Fulton AM, Laterra JJ, Hanchin CM. (1989). Prostaglandin E2 receptor heterogeneity and dysfunction in mammary tumor cells. *J Cell Physiol* **139**: 93–99.

Hata AN, Breyer RM. (2004). Pharmacology and signaling of prostaglandin receptors: Multiple roles in inflammation and immune modulation. *Pharmacol Ther* **103**: 147–166.

Hoshino T, Tsutsumi S, Tomisato W, Hwang HJ, Tsuchiya T, Mizushima T. (2003). Prostaglandin E2 protects gastric mucosal cells from apoptosis via EP2 and EP4 receptor activation. *J Biol Chem* **278**: 12752–12758.

Inazawa J, Inoue J, Imoto I. (2004). Comparative genomic hybridization (CGH)-arrays pave the way for identification of novel cancer-related genes. *Cancer Sci* **95**: 559–563.

Johnsen JI, Lindskog M, Ponthan F, Pettersen I, Elfman L, Orrego A *et al*. (2004). Cyclooxygenase-2 is expressed in neuroblastoma, and nonsteroidal anti-inflammatory drugs